

# Adaptation of the Alphaproteobacterium *Rhodobacter sphaeroides* to stationary phase

Matthew McIntosh <sup>1\*</sup>, Katrin Eisenhardt,<sup>1†</sup>  
Bernhard Remes,<sup>1</sup> Anne Konzer<sup>2</sup> and  
Gabriele Klug <sup>1</sup>

<sup>1</sup>Institut für Mikrobiologie und Molekularbiologie, IFZ,  
Justus-Liebig-Universität, 35392, Giessen, Germany.

<sup>2</sup>Biomolecular Mass Spectrometry, Max-Planck-Institute  
for Heart and Lung Research, Bad Nauheim, Germany.

## Summary

Exhaustion of nutritional resources stimulates bacterial populations to adapt their growth behaviour. General mechanisms are known to facilitate this adaptation by sensing the environmental change and coordinating gene expression. However, the existence of such mechanisms among the Alphaproteobacteria remains unclear. This study focusses on global changes in transcript levels during growth under carbon-limiting conditions in a model Alphaproteobacterium, *Rhodobacter sphaeroides*, a metabolically diverse organism capable of multiple modes of growth including aerobic and anaerobic respiration, anaerobic anoxygenic photosynthesis and fermentation. We identified genes that showed changed transcript levels independently of oxygen levels during the adaptation to stationary phase. We selected a subset of these genes and subjected them to mutational analysis, including genes predicted to be involved in manganese uptake, polyhydroxybutyrate production and quorum sensing and an alternative sigma factor. Although these genes have not been previously associated with the adaptation to stationary phase, we found that all were important to varying degrees. We conclude that while *R. sphaeroides* appears to lack a *rpoS*-like master regulator of stationary phase adaptation, this adaptation is nonetheless enabled through the impact of multiple genes, each responding to environmental conditions and contributing to the adaptation to stationary phase.

## Introduction

In natural environments, bacteria rarely find constant conditions that sustain steady growth over long periods. Rather, the bacterial lifestyle typically consists of brief periods of feasting and extended periods of starvation-induced growth arrest (Hobbie and Hobbie, 2013; Bertrand, 2019). The general assumption is that bacteria replicate at a maximal rate so long as they are surrounded by low-stress conditions and have access to all the necessary growth-supporting substrates. At some point, limitations in such substrates are detected and the bacterial population responds by slowing replication and transitioning to a growth-arrested state known as the stationary phase. In natural environments, low nutrients are usually accompanied by harsh conditions. Hence, the initial sensing of nutrient limitation, even under low-stress laboratory conditions, triggers regulatory activity and growth adaptation. The outcome is a slow-down in the growth rate, plus an increased resistance to various abiotic stresses including oxidative stress, extreme pH, extreme temperature, osmotic stress and desiccation (Roope 2nd *et al.*, 2003). General adaptations to stationary phase include downsizing cell size, increasing the trehalose concentration in the periplasmic space, increasing the thickness of the peptidoglycan layer, reducing membrane fluidity, condensing the nucleoid and the transition of ribosomes into an inactivate state to reduce costly protein synthesis while maintaining a basal level of translation (Navarro Llorens *et al.*, 2010; Jaishankar and Srivastava, 2017; Prossliner *et al.*, 2018).

It is remarkable that the preparation for survival during stationary phase begins prior to the stationary phase, in what may appear as anticipation of harder times ahead (Chang *et al.*, 2002; Blom *et al.*, 2011; Yang *et al.*, 2014; Cheng *et al.*, 2016; Weiss *et al.*, 2016). How do the bacteria achieve this? The first step is generally thought to be a remodelling of their transcriptomes through diverse transcriptional regulators such as alternative sigma factors (Navarro Llorens *et al.*, 2010), which are capable of rapidly inducing changes in gene expression within minutes of detecting environmental change (Rolfe *et al.*, 2012; Remes *et al.*, 2017).

The alternative sigma factor RpoS serves as the paradigm for understanding the adaptation to stationary

Received 24 October, 2018; revised 30 August, 2019; accepted 18 September, 2019. \*For correspondence. E-mail matthew.mcintosh@mikro.bio.uni-giessen.de; Tel. (+49) 641 99 355 57; Fax. 0641 99 35549. †These two authors contributed equally to this work.

phase. In *Escherichia coli* and other  $\gamma$ -proteobacteria, the expression of RpoS is triggered by multiple abiotic stresses and by limitation in carbon as a nutrient source (Battesti *et al.*, 2011; Hengge, 2011). RpoS is essential for *E. coli* survival of stationary phase. As cells transition from exponential to stationary phase, RpoS accumulates and increasingly competes with the primary sigma factor ( $\sigma^{70}$ ) for the major RNA polymerase holoenzyme. This results in the positive regulation of about 500 genes (10% of the genome) (Hengge, 2011). Hence, while the primary sigma factor is responsible for transcription of genes involved in cell growth under optimal growth conditions, the alternative sigma factors are responsible for transcription of genes involved in adaptation to survival under abiotic stress or nutrient limitation.

Alternative sigma factors are also involved in Gram-positive bacteria, such as *Bacillus subtilis* and *Corynebacterium glutamicum*, which have a primary sigma factor (SigA) plus a set of alternative sigma factors, each with its own regulon dedicated to a specific set of stress conditions or nutrient limitation (Patek and Nesvera, 2011; Yang *et al.*, 2014). SigB, for example, promotes dispersal from the biofilm when nutrients become limited (Bartolini *et al.*, 2019).

Adaptation to the stationary phase does not only involve sigma factors and other protein regulators such as two-component systems (Hengge, 2009). Non-protein-coding genes also control gene expression during the transition to stationary phase (Mika and Hengge, 2013; Sedlyarova *et al.*, 2016; Weiss *et al.*, 2016). One example is the non-coding 6S RNA (Cavanagh *et al.*, 2010; Elkina *et al.*, 2017). 6S RNA shows growth phase-dependent expression, interacts with the primary sigma factor (sigma-70) and regulates transcription of many sigma-70-dependent genes including the *relA* gene encoding a synthase of ppGpp, a secondary messenger molecule capable of triggering the stringent response (Cavanagh *et al.*, 2010). In *E. coli*, ppGpp is central to the adaptation to stationary phase (Nystrom, 2003). These and many other examples all point to a consensus: bacteria typically undergo marked and complex changes during the transition from exponential to stationary phase. General mechanisms underlying this adaptation are still poorly understood, even in well-studied model organisms. For example, although the deletion of the *rpoS* gene in *Salmonella typhimurium* reduced survival during stationary phase, this effect was lost when cells were grown anaerobically (Testerman *et al.*, 2002), indicating that RpoS and its regulon may be specific to protection against oxidative stress rather than nutrition-depletion induced adaptation to stationary phase (Nystrom, 2003).

Even less is known about the adaptation of the  $\alpha$ -proteobacteria to the stationary phase. *Rhodobacter*

*sphaeroides*, a well-studied member of the  $\alpha$ -proteobacteria, is a free-living facultative anoxygenic phototroph. Its natural habitat is anoxic waters and underwater mud. Regulatory mechanisms underlying the switch between different metabolic pathways and the adaptation to oxidative and photo-oxidative stress have been intensively studied. Like other  $\alpha$ -proteobacteria, *R. sphaeroides* does not contain a RpoS homologue with comparable functions to RpoS of enteric bacteria (Staron and Mascher, 2010). It does contain genes for numerous alternative sigma factors, and some of these have been well studied. For example, the sigma factor  $\sigma$  (EcfG) along with its anti- $\sigma$  factor NepR and the anti-anti- $\sigma$  factor PhyR are present in *R. sphaeroides*. These genes are thought to be important for the general stress response in many  $\alpha$ -proteobacteria (Fiebig *et al.*, 2015). In *R. sphaeroides*, however, PhyR does not play a major role in either oxidative stress or the general stress response, but rather has a more specialized role in defense against specific membrane stress factors (Li *et al.*, 2018). Other alternative sigma factors in *R. sphaeroides* include the RpoH1 and RpoH2 proteins, which are important for protection against a variety of stresses including oxidative stress, photooxidative stress and heat stress, and are shared by various members of the  $\alpha$ -proteobacteria (Delory *et al.*, 2006; Martinez-Salazar *et al.*, 2009; Nuss *et al.*, 2009; de Lucena *et al.*, 2010; Barnett *et al.*, 2012; Dufour *et al.*, 2012). Both RpoH1 and RpoH2 have a major role during the transfer to fresh medium from stationary phase (Remes *et al.*, 2017), since this environmental condition induces an oxidative stress response (Cuny *et al.*, 2007).

Here, we focus on the exponential-to-stationary phase transition to learn how *R. sphaeroides* adjusts its gene expression during this stage. We documented changes in the transcriptome and the proteome during the growth phases under both low and highly aerated conditions and identify a small set of genes based upon two criteria: those that clearly change expression upon entry into the transition phase, and whose change is independent of oxygen levels. Under a working hypothesis that the timing of gene expression can provide hints about function, we tested a set of four of these candidate genes for their effect on growth during the adaptation to stationary phase. To achieve this, we have developed a novel setup, which includes a suicide vector to selectively alter gene expression, a low copy plasmid for monitoring promoter::reporter expression activity and an automated assay to monitor growth and promoter activity in 96-well plate cultures at 1 h intervals. Furthermore, by changing environmental conditions and using growth and promoter activity as a readout, this approach revealed that once the influence of oxygen on gene expression has been taken into account, the number of gene expression

changes that accompany the adaptation to stationary phase by *R. sphaeroides* are small but important for growth.

## Results and discussion

### Transcriptome analysis

To learn how the *R. sphaeroides* transcriptome changes during the transition phase, we grew *R. sphaeroides* 2.4.1 in a defined salts medium containing malate as the carbon source (Remes *et al.*, 2014). The growth phases were broadly decipherable from the growth curves (Fig. 1) and are as follows: exponential phase, OD 0.4–0.45, transition from exponential to stationary phase, OD 0.9–1.2, early stationary phase, OD 1.7–2.0, and outgrowth, OD 0.2. In this setup, the outgrowth is defined as the phase of growth 20 min after the cells from the stationary phase were diluted in fresh medium. The transition phase is defined as the initial slow-down in growth (starting at OD 0.9) immediately following the exponential phase and prior to the stationary phase. Samples for RNA isolation were collected at the sampling points, indicated as red points, in the growth plots (Fig. 1).

Extracted RNA used for microarray analysis (MA) was based upon two arrays, each with RNA pooled from three independent biological replicates. The reproducibility of microarray replicates was very high, as reflected by Pearson correlation ( $r$ ) ranging between 0.96 and 0.98 (Remes *et al.*, 2017). Genes were classified according to their relative RNA levels in the different growth phases. This was determined by comparison to the level in the exponential phase as the baseline (see Fig. S1 for an overview of transcript changes). Fold changes of  $\geq 2$  or

$\leq -2$  were used as a cut-off to define the transcripts with changed levels. Our analysis was based on the detection of mRNA from 4390 genes with a reliable A-value (average signal intensity for a gene across all arrays) in the transition phase samples.

Anoxygenic phototrophic bacteria are rarely found in natural environments with continuous high aeration, and it is known that the expression of many genes is influenced by the oxygen level (Gregor and Klug, 2002; Zeilstra-Ryalls and Kaplan, 2004). Hence, we analysed cultures under both low and highly aerated conditions. This was ensured by using 500 ml Erlenmeyer flasks containing 400 ml of defined medium for low aerated cultures and 500 ml baffled flasks with 125 ml for highly aerated cultures. In the low aerated cultures (Fig. 1A), oxygen levels dropped rapidly from 75% to 1%–2% (25–30  $\mu\text{M}$ ) within 5 h, the time needed for the first doubling (from OD 0.2 to OD 0.4).

It then stayed consistently low for another 5 h until OD of about 1.0. After reaching this OD, growth slowed and oxygen saturation increased to about 70% at 24 h after inoculation (Fig. 1A). In highly aerated culture conditions, the oxygen levels remained between 95% and 100% (160–180  $\mu\text{M}$ ) saturation (Fig. 1B). The growth curves did not greatly differ between the two conditions.

### Carbon is the growth limiting factor

It is commonly assumed that limitation in nutrients or oxygen slows down growth and forces bacterial cultures to adopt a stationary phase. Our results indicated that oxygen levels had a minimal effect on the timing of entry into the stationary phase for chemotrophically growing *R. sphaeroides* cells (Fig. 1). To establish which factor limits

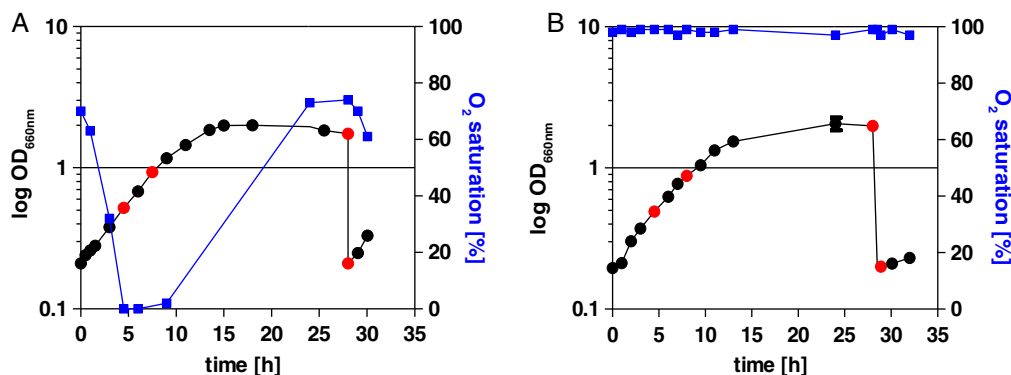


**Fig. 1.** Growth curves and oxygen levels. *Rhodobacter sphaeroides* wild type 2.4.1 was grown under low aerated (A) or highly aerated (B) conditions and measurements of oxygen levels and growth (optical density at 660 nm ( $\text{OD}_{660}$ )) were recorded. Pre-cultures used for inoculation were grown under low aeration to an  $\text{OD}_{660}$  of 0.6–0.7, which is near the end of the exponential phase, and then diluted to an  $\text{OD}_{660}$  of 0.2 with fresh medium. The dilution step is represented by 0 h in Fig. 1A and B.  $\text{OD}_{660}$  was determined over time and is represented by a black line. The  $\text{OD}_{660}$  is presented on a logarithmic scale ( $\log_2$ ) to distinguish the exponential phase from the transition phase. For both conditions, the end of the exponential phase occurs at  $\text{OD} = 1$ . The oxygen saturation (blue) is presented in percent. Time points when RNA samples were taken for microarray analysis are indicated as red dots. Both data sets represent the mean of at least three independent experiments and error bars represent standard deviation (although these are only visible for a few time points, since reproducibility was high).

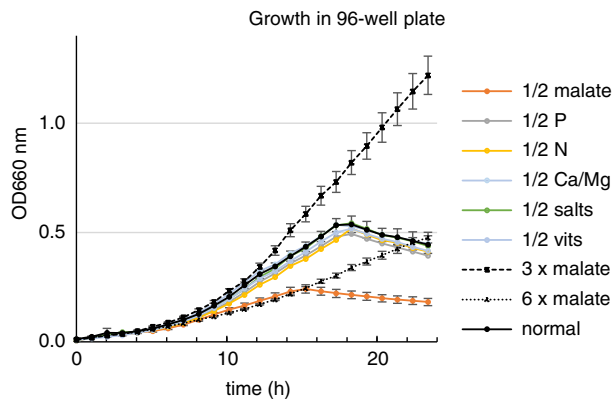


**Fig. 2.** Malate is the growth-limiting factor. Growth of *R. sphaeroides* was monitored ( $OD_{660}$ ) over 24 h during growth in a modified defined medium. Defined medium (see Table S2) was modified by dilution (1:2) with water followed by further alterations as follows: each of the medium constituents were methodically altered by halving the concentration or, in the case of malate, by increasing the concentration by threefold or sixfold, as indicated in the legend. Phosphate (P),  $K_2HPO_4/KH_2HPO_4$ ; nitrogen (N),  $NH_4Cl$ ; calcium and magnesium (Ca/Mg),  $CaCl_2/MgSO_4$ ; salts, trace elements (see Table S2) plus  $FeC_6H_6O_7$ ; vitamins (vits), thiamine, niacin, nicotinamide and biotin. The media were inoculated at  $OD_{660\text{ nm}}$  of 0.01 and incubated in 0.1 ml volumes in a 96-well plate. This 96-well plate was continuously shaken and incubated at 32 °C in a Tecan Infinity plate reader which measured  $OD_{660\text{ nm}}$  at 60 min intervals for 24 h. OD is shown on a linear scale to better visualize differences in growth caused variations in the medium constituents. Error bars represent the standard deviation for eight independent cultures.

growth in the minimal salts medium containing malate as the carbon source, we tried to enhance growth by increasing the concentration of each of these constituents of the minimal medium, e.g., malate, trace elements, iron, vitamins, phosphate, calcium and magnesium, but none of these additions enhanced growth (data not shown). We then employed a different strategy. First, the standard culture medium was diluted 1:2 with water so that each constituent was present at 33% (v/v). Then, a series of media were prepared, each differing in one aspect: one or a set of related ingredients (e.g., trace elements or vitamin cocktail) was further reduced by one-half (i.e., to 16.5%). Upon inoculation with *R. sphaeroides*, cultures were grown in 0.1 ml volumes in a 96-well plate. Figure 2 shows the growth of these cultures ( $OD_{660\text{ nm}}$ ) plotted on a linear scale (rather than a logarithmic scale) to better visualize the differences in growth and reveals that malate is indeed the limiting factor for growth. Decreasing the malate level to 16.5% (1/2 malate) clearly limited growth, while decreases in each of the other constituents did not affect growth. The addition of malate (3× malate) improved growth (this concentration of malate represents the malate level in the undiluted standard medium), while even higher levels (6× malate) considerably slowed growth. Thus, these results indicate that growth in this defined medium is limited by malate abundance.

### Influence of oxygen levels on induction of genes in the transition phase

Oxygen levels are capable of influencing gene expression in *Rhodobacter* (Gregor and Klug, 2002; Zeilstra-Ryalls and Kaplan, 2004). Our global analysis revealed those genes whose transcript levels were influenced by oxygen. From the 4390 genes with reliable A-values in the microarray analyses, less than 10% showed oxygen-dependent changes of  $\geq$ twofold ( $\log_2$  fold change  $\geq 1$ ) in the transition phase (Fig. S1). Genes with decreased transcripts in the transition phase amounted to 241 under highly aerated conditions, and 179 under low aerated conditions. Many of the genes with decreased transcripts belong to the COG-C category, representing energy metabolism and conversion, COG-H for coenzyme transport and metabolism, and COG-I for lipid transport and metabolism. The subset of genes with decreased transcripts in the transition phase by the presence of oxygen provide further support for the reliability of our data since this set of genes include not only genes responsible for photosynthesis (Fig. S2) but also *cco* genes (*cbb3* type cytochrome oxidase), *feoA* and *feoB* ( $Fe^{2+}$  transport), *nuo* genes (NADH dehydrogenase), and genes for some other metabolic enzymes that are known to strongly depend on the redox conditions (Zeilstra-Ryalls and Kaplan, 2004; Arai *et al.*, 2008; Remes *et al.*, 2017).

Genes with  $\geq$ twofold increased transcript levels in the transition phase amounted to 30 under highly aerated conditions and 55 under low aerated conditions. Because we were interested in those transcripts that were important for the adaptation to the stationary phase regardless of the oxygen levels, we looked for genes showing  $\geq$ twofold changes in transcript levels under both low and highly aerated conditions. Only 12 genes with increased transcripts in the transition phase reached this cut-off, suggesting that most of the changes were related to oxygen levels and were not specific to the adaptation to stationary phase. Similarly, only 60 genes showed a decrease in transcripts in the transition phase under both low and highly aerated conditions. Thus, based on this approach, we identified a relatively small number of genes (60 down, 12 up) that showed changed transcript levels during the transition phase independently of aeration. These are listed in Table 1. We included in Table 1 another gene, RSP\_0557, whose transcript levels also increased in the transition phase, along with the other 12 genes. However, RSP\_0557 transcript levels did not reach the  $\geq$ twofold increase cut-off under low aerated conditions and is therefore included in Table 1 as an exception (see below). The total transcriptome data set, along with COG assignments, is provided in Table S1.

Since we were interested in learning how *R. sphaeroides* adapts to the stationary phase, we postulated

Table 1. Genes with changed expression specific to the transition phase.

Locus	Function	Gene	Microarray (low aerated)			Microarray (high aerated)			RNAseq			Proteome		
			trans	stat	lag	trans	stat	lag	trans	stat	lag	trans	stat	lag
<b>RSP_0904</b>	ABC Mn transporter, periplasmic substrate-binding protein	<i>sitA</i>	2.9	1.8	0.3	1.6	0.4	-1.4	4.2	-1.0	3.5	3.2		
RSP_3453	TRAP-T family transporter, periplasmic binding protein		1.9	-0.1	0.1	1.4	0.8	0.1	2.9	-0.2	2.0	1.5		
RSP_3746	Hypothetical protein		1.5	0.1	-0.2	1.2	0.7	0.0	3.0					
<b>RSP_0123</b>	Autoinducer synthesis protein	<i>cerI</i>	1.5	0.3	-1.3	1.3	-0.7	-2.2	1.5	-1.0	-2.3	0.1		
RSP_0850	Hypothetical protein		1.5	1.2	0.0	1.5	1.8	0.4	3.1	1.8	2.8	2.7		
RSP_6042	Hypothetical protein		1.5	1.2	0.2	1.3	2.1	0.5	1.0					
RSP_3747	Putative dipeptidase		1.4	0.2	0.1	1.1	0.9	0.2	2.9	0.1	2.2	2.1		
RSP_3456	Dihydrodipicolinate synthase		1.4	-0.1	0.1	1.2	0.2	0.2	2.3	-0.2	1.0	1.1		
<b>RSP_0381</b>	Putative phasin	<i>phaP</i>	1.3	-1.3	-0.2	1.5	-1.4	0.2	1.3	0.8	1.0	0.7		
<b>RSP_6037</b>	Hypothetical protein, DUF1127 domain		1.2	-1.4	-1.2	3.1	-0.5	2.3	2.1					
RSP_3093	Predicted integral membrane protein		1.2	0.0	-0.5	1.5	0.2	0.4	1.1	1.5	3.3	2.7		
<b>RSP_3095</b>	Putative RNA polymerase sigma-70 factor		1.0	1.5	-0.1	2.0	2.6	0.7	1.8					
<b>RSP_0557</b>	Hypothetical protein, DUF1127 domain		0.8	-1.6	-0.8	2.4	-1.1	1.7	1.6					
RSP_0296	Cytochrome c <sub>2</sub>	<i>cycA</i>	-2.5	-1.1	-2.1	-1.2	-0.2	-0.7	-1.2	1.4	0.7	0.2		
RSP_1951	Hypothetical protein		-2.3	0.2	0.4	-3.6	-4.3	-0.6	-0.5					
RSP_0910	TRAP-T family transporter, C4-dicarboxylate-binding	<i>dctP</i>	-2.1	-0.8	-0.4	-3.3	-3.2	-2.4	-2.6	0.0	-0.3	-0.4		
RSP_0912	TRAP-T family C4-dicarboxylate transporter	<i>dctM</i>	-2.0	-0.3	-0.1	-2.8	-2.9	-2.5	-3.1	0.3	0.0	0.4		
RSP_3751	Hypothetical protein		-2.0	-0.1	-1.2	-1.7	-1.6	-0.6	-3.5	0.2	-0.2	-0.2		
RSP_0911	TRAP-T family C4-dicarboxylate transporter	<i>dctQ</i>	-1.9	-0.5	-0.1	-2.9	-3.1	-2.6	-2.6	-0.3	-0.5	0.0		
RSP_3622	Hypothetical protein		-1.9	0.1	0.3	-3.2	-3.9	-0.7	0.2					
RSP_2299	ATP synthase subunit B (EC:3.6.3.14)	<i>atpD</i>	-1.7	-0.6	0.1	-2.0	-3.3	-0.3	-1.1	0.1	-0.4	-0.4		
RSP_3750	Hypothetical protein		-1.7	-0.3	-1.0	-1.2	-1.2	-0.5	-2.5	0.2	-0.4	-1.1		
RSP_2200	Transcriptional regulator, MerR family		-1.7	-0.2	-1.2	-1.5	-1.1	-0.4	-1.0					
RSP_1035	FoF1 ATP synthase	<i>atpF</i>	-1.6	-0.9	0.4	-2.4	-3.6	0.0	-1.4	0.2	0.0	0.1		
RSP_3539	Hemolysin-type calcium-binding region, RTX		-1.6	-0.1	0.0	-2.0	-2.9	-1.5	-0.9	-1.5	-2.0	0.4		
RSP_0696	Cbb3-type cytochrome oxidase CcoN subunit	<i>ccoN</i>	-1.6	-0.5	-1.9	-1.3	-3.0	-1.6	-2.0	-0.1	0.1	-0.2		
IGR_2750_s			-1.6	-2.2	1.1	-1.1	-0.6	1.1	-					
RSP_6094	TRAP-T sorbitol/mannitol transporter, DctM subunit	<i>ivdH</i>	-1.6	-0.7	0.3	-2.9	-3.3	-1.7	-2.0	-0.5	-0.7	-0.5		
RSP_2506	Isovaleryl-CoA dehydrogenase (EC:1.3.99.10)		-1.5	0.1	-0.9	-1.7	-2.6	-2.4	-0.2	1.8	1.6	1.6		
RSP_3231	ABC peptide transporter, periplasmic binding protein	<i>Pnp</i>	-1.5	-0.9	-1.9	-1.8	-2.8	-1.3	-1.2	0.6	0.5	0.2		
RSP_1112	Polyribonucleotide nucleotidyltransferase (EC:2.7.7.8)		-1.5	-0.3	1.0	-2.3	-3.1	0.5	-1.1	0.0	-0.5	0.0		
RSP_0099	TRAP-T sorbitol/mannitol transporter, DctQ subunit	<i>atpE</i>	-1.5	-0.4	0.2	-3.0	-3.3	-1.7	-2.1	0.4	-0.1	0.2		
RSP_1037	ATP synthase subunit C (EC:3.6.3.14)	<i>hemZ</i>	-1.5	-0.7	0.2	-2.1	-3.9	-0.1	-1.2					
RSP_0699	Coproporphyrinogen III oxidase		-1.5	0.0	-1.4	-1.2	-2.1	-1.8	-3.0	0.7	-0.1	-4.0		
IGR_0423_s			-1.5	-0.5	0.1	-3.1	-4.8	-0.9	-					
RSP_2300	ATP synthase, delta/epsilon subunit (EC:3.6.3.14)	<i>atpC</i>	-1.4	-1.7	0.2	-1.9	-3.1	-0.4	-1.4	0.3	0.1	0.2		
RSP_1036	FoF1 ATP synthase	<i>atpX</i>	-1.4	-1.3	0.3	-2.4	-4.2	0.1	-1.9	0.6	0.0	0.4		
RSP_0154	3-hydroxyisobutyrate dehydrogenase (EC:1.1.1.31)		-1.4	-0.3	-0.7	-1.2	-1.1	-0.9	-1.5	1.2	0.5	0.1		
RSP_1354	Beta-ketothiolase (EC:2.3.1.9)		-1.3	0.0	-0.9	-1.4	-1.3	-1.1	-1.0	1.0	0.9	0.8		
RSP_3587	<i>N</i> -(5'-phosphoribosyl) anthranilate isomerase		-1.3	-0.6	-1.4	-1.1	-0.9	-0.7	-1.9	0.7	0.0	0.0		
RSP_0741	Putative metallo-beta-lactamase family protein		-1.3	0.0	-0.8	-1.0	-0.8	-0.7	-2.0	0.6	-1.5	-1.3		

(Continues)

Table 1. Continued

Locus	Function	Gene	Microarray (low aerated)			Microarray (high aerated)			RNAseq			Proteome		
			trans	stat	lag	trans	stat	lag	trans	stat	lag	trans	stat	lag
RSP_2508	Methylcrotonyl-CoA carboxylase beta chain (EC:6.4.1.4)	<i>mccB</i>	-1.3	0.0	-0.4	-1.1	-1.3	-1.4	-0.3	2.0	1.9	1.7		
RSP_4045	Fructose-bisphosphate aldolase (EC:4.1.2.13)	<i>fabB</i>	-1.3	-0.6	-0.4	-1.1	-2.6	-0.8	-0.6	-0.1	-0.2	0.0		
RSP_0711	Hypothetical protein	<i>YbaB</i>	-1.3	-0.3	-0.4	-1.6	-1.8	-0.5	-1.1	0.6	0.1	0.1		
RSP_0577	Hypothetical protein		-1.3	-0.1	-1.2	-1.4	-1.1	-0.9	-0.6					
RSP_1690	Electron transfer flavoprotein, alpha subunit	<i>etfA</i>	-1.2	-0.1	-0.3	-1.2	-1.6	-0.6	-0.9	0.4	-0.2	-0.3		
RSP_1691	Electron transfer flavoprotein beta-subunit	<i>etfB</i>	-1.2	0.0	-0.4	-1.5	-1.9	-0.6	-1.3	0.7	0.2	0.1		
IGR_0360_as			-1.2	-0.2	-1.1	-1.1	-2.7	-1.9	-					
RSP_1140	Branched-chain amino acid aminotransferase	<i>ilvE</i>	-1.2	0.2	-1.2	-1.9	0.4	0.5	-0.9	0.3	0.0	0.0		
RSP_2509	Methylcrotonyl-CoA carboxylase alpha chain	<i>mccA</i>	-1.2	-0.2	-0.4	-1.4	-1.7	-1.5	-0.6	2.1	1.8	1.6		
RSP_3540	Putative adhesin or RTX toxin		-1.2	-0.1	0.1	-1.0	-1.7	-0.6	-					
RSP_4355	(rRNA)	23S	-1.2	-1.4	-0.6	-1.8	-2.8	-0.3	0.7	-0.1	0.0	-0.1		
RSP_2283	30S ribosomal protein S4	<i>rpsD</i>	-1.2	-0.6	0.8	-2.2	-3.9	-0.3	-1.0					
RSP_4342	(miscRNA)	<i>rnpB</i>	-1.1	-0.5	-1.1	-1.6	-1.3	-1.8	-					
RSP_0097	TRAP-T sorbitol/mannitol transporter	<i>takP</i>	-1.1	-0.5	-0.7	-2.4	-2.9	-2.2	-0.1	0.3	-0.1	-0.2		
RSP_2298	ATP synthase subunit C (EC:3.6.3.14)	<i>atpG</i>	-1.1	-0.8	0.1	-1.4	-2.0	-0.2	-0.8	-0.4	-0.8	-0.6		
RSP_1952	Cold-shock DNA-binding domain protein		-1.1	-0.6	0.0	-2.7	-4.4	-1.1	0.4					
IGR_1486_s			-1.1	0.2	0.0	-1.5	0.9	-0.6	-					
RSP_3620	Cold-shock DNA-binding protein		-1.1	-0.1	0.1	-2.6	-4.2	-1.0	0.3					
RSP_4295	(rRNA)	23S	-1.1	-1.3	-0.5	-1.8	-2.8	-0.9	0.7					
RSP_0007	Putative outer membrane protein		-1.1	-0.1	-0.8	-1.2	-1.2	-0.7	-0.5	0.7	0.4	0.0		
RSP_3985	Hypothetical protein		-1.1	-0.7	-0.1	-1.3	-1.5	-0.6	-1.6	0.2	0.1	0.3		
RSP_3621	Cold-shock DNA-binding protein		-1.1	-0.6	-0.1	-2.6	-4.8	-1.2	0.4					
RSP_2463	Acyl carrier protein	<i>acpP</i>	-1.0	-0.7	0.3	-1.8	-3.2	-0.4	-0.9	-0.5	-0.4	-0.3		
RSP_0625	Putative Maf-like protein		-1.0	-0.2	0.3	-1.1	-1.5	-0.3	-1.7	-0.1	-0.1	-0.1		
RSP_1038	ATP synthase subunit A (EC:3.6.3.14)	<i>atpB</i>	-1.0	-0.4	0.3	-1.5	-2.5	0.2	-1.2	-1.1	-1.1	-0.5		
RSP_1048	30S ribosomal protein S16	<i>rpsP</i>	-1.0	-1.1	0.3	-1.5	-2.6	0.1	0.3	0.5	0.0	0.2		
RSP_1723	50S ribosomal protein L16	<i>rplP</i>	-1.0	-1.4	0.5	-1.5	-3.0	-0.3	-0.4	-0.1	-0.4	-0.4		
RSP_2710	Putative membrane-associated zinc metalloprotease		-1.0	-0.1	-0.5	-1.2	-1.2	-0.1	-1.1	0.3	-0.5	-0.1		
RSP_0147	Glutamine synthetase class-1 (EC:6.3.1.2)	<i>glnA</i>	-1.0	-1.0	-0.5	-1.1	-2.6	-0.4	-0.3	-0.3	-0.6	-0.3		
RSP_0968	Malate dehydrogenase (EC:1.1.1.37)	<i>mdh</i>	-1.0	-0.3	-0.1	-1.1	-1.8	-0.5	-1.4	0.1	-0.3	-0.3		
RSP_1721	50S ribosomal protein L22	<i>rplV</i>	-1.0	-0.8	0.3	-1.5	-3.5	-0.3	-0.8	0.2	0.4	0.3		

Bold values indicate candidate transcripts whose levels were either above or below the cut-offs of 1.0 or -1.0, respectively, in the transition phase. The inclusion of these genes is based upon two criteria: (i) RNA levels are changed by twofold ( $\log_2FC$  of >1 or <-1, all values listed are  $\log_2FC$  changes) in the transition phase compared with the exponential phase, and (ii) the increase in the transition phase is observable under both low and highly aerated conditions. Together, these criteria mean that the change is specific to the transition phase. (RSP\_0557 is included among the genes with increased transcripts in the transition phase as an outlier. It did not reach the  $\log_2FC$  of >1 under low aerated conditions.) The data are based on the MA, with the mass spectrophotometry proteome analysis and RNAseq analysis providing complementary data. Proteomic and RNAseq analyses were performed only on samples from low aerated cultures. Growth phases are represented by trans (stationary phase) and lag (lag phase or outgrowth). For IGRs (intergenic regions), s = sense, as = antisense.

that mRNAs with increased levels in the transition phase are of primary interest. Almost half of these are for hypothetical proteins, and most have never been investigated for functionality (Table 1). For the remainder of this investigation, we focused on the 12 genes with oxygen-independent increased transcript levels in the transition phase. Transcript levels of most of these were highest in the transition phase, and then returned to lower levels in the stationary phase. The single clear exception to this pattern was RSP\_3095, coding for an alternative sigma factor. Its transcript levels continued to increase in the stationary phase under both low and highly aerated conditions. Also of interest is the presence of another gene, RSP\_6037, which was previously shown to be involved in the stress response (Billenkamp *et al.*, 2015). Both RSP\_6037 and the above-mentioned RSP\_0557 code for DUF1127 proteins. Their transcripts were the most strongly induced mRNAs in the transition phase under highly aerated conditions. The promoters of both RSP\_6037 and RSP\_0557 were previously shown to be controlled by the RpoHI/HII sigma factors, which induces expression in response to singlet oxygen (Berghoff *et al.*, 2013).

#### Confirmation of increased transcripts of the transition phase

To increase confidence in the finding that these transition phase candidates have changed transcripts levels, we subjected extracted RNA from low aerated cultures for RNAseq (single run from biological triplicates). This analysis confirmed all 12 genes, plus RSP\_0557, as having  $\geq$ twofold increased transcripts levels in the transition phase (Table 1). We also analysed mRNA levels of some of these genes via RT-qPCR (Fig. 3A). Here,  $\log_2$  fold change values represent the changes in mRNA abundance at each time point (8, 11 and 28 h) relative to total mRNA abundance in the early exponential phase (4 h). In this experiment, 8 h was near the end of the exponential phase, 11 h was in the middle of the transition phase and 28 h represents the stationary phase. Transcripts from RSP\_6037 (DUF1127), *sitA* (first gene in the *sitABCD* operon which putatively codes for a manganese uptake transporter), *cerI* (coding for a quorum-sensing pheromone synthase), and RSP\_0381 (putatively coding for a phasin, PhaA) were confirmed via RT-qPCR to increase in the transition phase (11 h). RT-qPCR also confirmed that high-aerated conditions promote the increase in mRNA levels of RSP\_6037 and RSP\_0557. RSP\_6037 is co-transcribed with the *ccsR1-4* genes for a set of highly homologous sRNAs (Billenkamp *et al.*, 2015). This gene cluster is thought to be essential (cannot be deleted) and is involved in various stress responses of *R. sphaeroides* by affecting the

C1-metabolism and the pyruvate dehydrogenase complex (Billenkamp *et al.*, 2015). We confirmed that one of the sRNAs, CcsR3, increased strongly in the transition phase via Northern analysis (Fig. 3B). Altogether, these results from microarray, RNAseq, RT-qPCR and Northern analysis indicated a high level of reliability in transcript detection.

#### Promoter-reporter fusions revealed distinct expression profiles during the transition to stationary phase

Up to this point, our analysis was based upon the detection of changes in mRNA levels. To learn how the promoter activity of selected genes changes throughout the growth phases, we employed an additional approach by fusing the upstream region of each gene (300–400 bp, including the promoter, translation start and 3–5 following codons) to the gene for the mVenus fluorescence protein. The advantage of this approach is that the accumulation of mVenus protein provides an approximation of gene expression, i.e., the total output from the combined steps of transcription and translation. In addition to the promoters of the genes listed above, we included the promoters of several other genes. The criteria for their selection were on the basis of having a previously established essential role in growth, either in *R. sphaeroides* or whose homologues have been studied in various other  $\alpha$ -proteobacteria. These included the promoter of *dnaA*, an essential gene coding for the master regulator of chromosomal replication in almost all bacteria (Katayama *et al.*, 2010) and the promoter of *mraZ*, the first gene in a cell division gene cluster that includes *ftsZ* that is essential for cell division in most bacteria (Ortiz *et al.*, 2016). We also included the promoter of *rpoZ*, coding for the omega subunit of the RNA polymerase present in all free-living bacteria (Weiss and Shaw, 2015). *rpoZ* is also co-transcribed with the downstream *relA* gene that codes for the ppGpp synthase in *S. melliloti* (Krol and Becker, 2011), and the *R. sphaeroides* *rpoZ-relA* locus shares a similar genetic topology. Other promoters included in our analysis are the promoter of *rpoHI*, coding for an alternative sigma factor (Remes *et al.*, 2017), the promoter of *takP*, a TRAP transporter for the uptake of carbon (Adnan *et al.*, 2015) and the promoter of the 16S rRNA gene, previously used in *R. sphaeroides* for the strong constitutive overexpression of target genes (Mank *et al.*, 2012). In the cases of the *dnaA*, *mraZ* and *rpoZ* fusions, their native ribosome binding sites (RBS) were replaced by that of *cerI*, since preliminary data (not shown) revealed that the *cerI* RBS was very efficient. Similarly, the *cerI* RBS was used in the fusion of the 16S promoter to the gene for mVenus. The *R. sphaeroides* wild type strain carrying the promoter-mVenus fusions was grown in a 96-well plate and

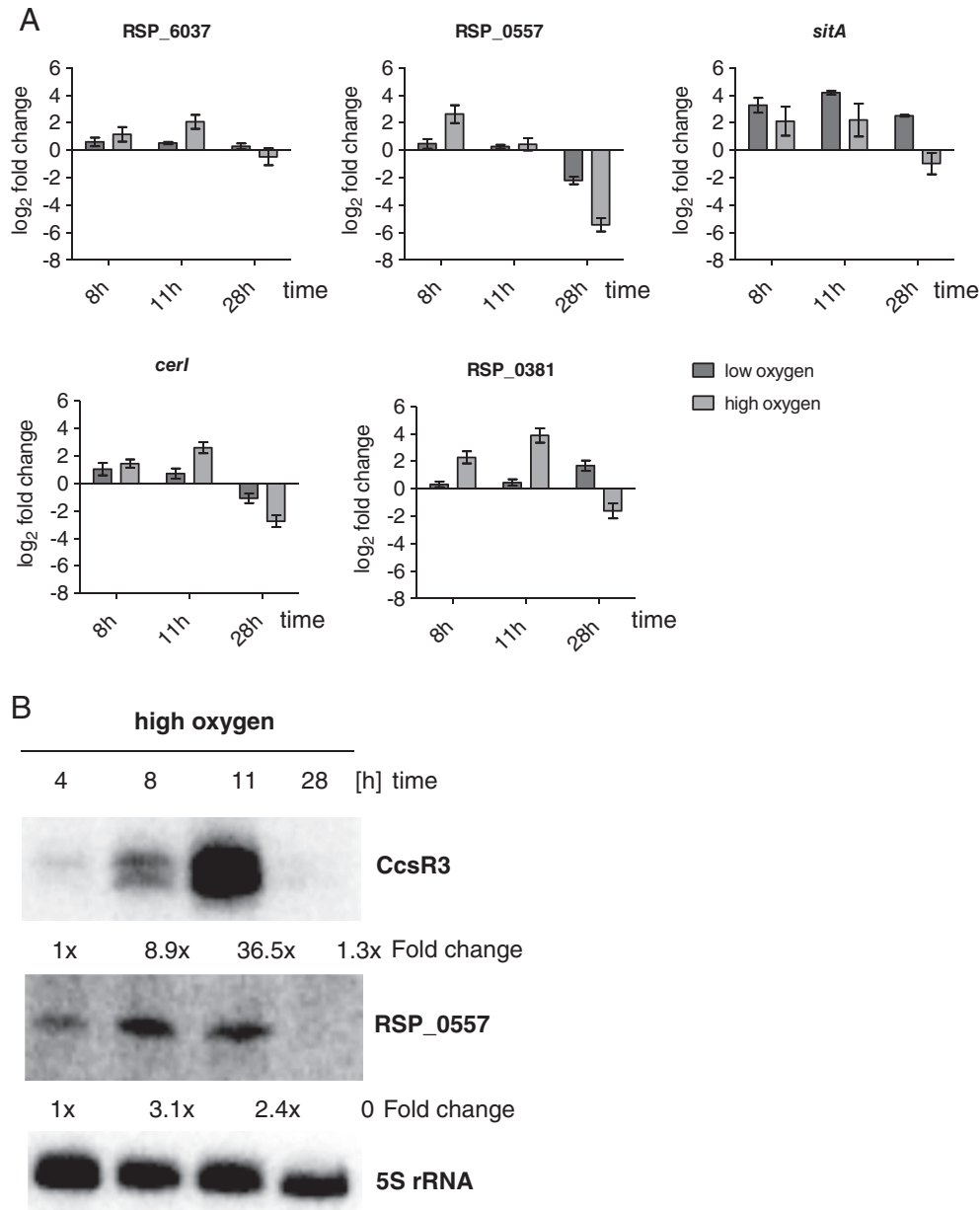


**Fig. 3.** mRNA levels change according to the growth phase. Transcript levels of selected genes were detected via (A) real-time RT-qPCR and (B) Northern analysis. For the RT-qPCR, log<sub>2</sub> fold change values represent the changes in mRNA abundance at each time point relative to total mRNA abundance in the early exponential phase (4 h). The bars represent the average of biological triplicates with technical duplicates, and error bars indicate the standard deviation. B. Northern blot analysis. Numbers below each blot indicate fold change relative to the first time point (4 h, early exponential phase).

fluorescence and optical density was automatically measured at 1 h intervals for up to 24 h. Under these conditions, the growth phases were observable as follows: exponential phase (4–13 h), transition phase (13–18 h) and stationary phase (>18 h) (Fig. 4A). Interestingly, of the 12 different promoters included in this analysis, two distinct classes emerged. The first class (Class I) included PdnaA, PmraZ, PcerI, PphaP, PtaKp and P16S (Fig. 4B). The activity of these promoters was low during the lag phase, high during the exponential phase and

then low again during the transition phase (indicated by the lack of increase in fluorescence, F). Notably, the activity of these promoters is virtually exclusive to exponential growth. A second group of promoters (Class II) showed a variety of activity profiles (Fig. 4C). For example, P*sitA* was activated in the mid exponential phase, and this matched well with the microarray data (Table 1) and the RT-qPCR data (Fig. 3A). Other notable Class II promoters include that of RSP\_0557 and the putative alternative sigma factor, RSP\_3095, whose expression

clearly increased upon entry into the transition phase. Most of the promoter activity profiles matched well with the MA (see Table 1), although some minor differences were apparent, e.g., *PcerI* and *PphaA*. These promoters were active in the exponential phase but not in the transition phase (Fig. 4B), in contrast to their transcript accumulation patterns (Table 1, Fig. 3A and B).

#### *Impact of selected genes on growth*

We wanted to learn how the genes with increased transcripts identified in our MA impacted growth and adaptation to stationary phase. Therefore, we selected candidates from the 12 genes, which showed increases in transcript levels in the transition phase and altered their expression via targeted insertions of the suicide plasmid pK18mobII (see Materials and Methods for details and Fig. S3 for explanatory diagram). The genes that we focused on were *sitA*, *phaA*, *cerI* and the uncharacterized sigma factor RSP\_3095. We chose these because predictions about their functions were available and because related genes in other bacteria are known to impact growth. Our expectation was that if these genes were important for the adaptation of *R. sphaeroides* to the stationary phase, the alteration of their expression (either knockdown or constitutive expression) ought to disturb growth and adaptation to stationary phase.

#### *sitABCD expression reveals the importance of Mn for growth*

The genes with the most strongly increased transcripts in the transition phase are from an operon that encodes the subunits of the putative manganese (Mn) ABC transporter, SitABCD (Table 2, Fig. 4C). Mn is an essential micronutrient for all forms of life (Kehres and Maguire, 2003). Some bacteria even have multiple Mn uptake systems. *Enterococcus faecalis*, for example, has three Mn uptake systems, at least two of which are dedicated to Mn uptake (Colomer-Winter *et al.*, 2018). The knockout of all three systems resulted in poor growth. Furthermore, Mn depletion triggered ppGpp accumulation and the stringent response. Normal growth of a ppGpp<sup>0</sup> mutant of *E. faecalis* in a defined medium with low Mn levels could be restored by the addition of Mn. The authors concluded that Mn has an important role in the adaptation to nutrient limitation and in coping with high levels of endogenously produced reactive oxygen species (Colomer-Winter *et al.*, 2017).

To learn whether the expression of *sitABCD* was important for *R. sphaeroides*, we measured growth and PsitA activity in the presence of varying Mn levels in the defined growth medium. When no manganese was added to the medium (0 nM), the bacterium grew poorly (Fig. 5A) and showed strong PsitA activity from 2 h after

inoculation and onwards (Fig. 5B). Presumably, the weak growth that was observable was due to the presence of background levels of Mn. The addition of manganese at the standard concentration of 45 nM reproduced the delayed activation of PsitA at around 8 h after inoculation. A higher concentration (90 nM) further delayed the activation by 2 h, while concentrations of 225 and 450 nM resulted in a complete lack of activation of PsitA (Fig. 5B). This result indicates, first, that the presence of Mn is important for growth, second, that the Sit operon expression appears to be activated only when Mn becomes scarce.

The situation was different when the transcription of the *sitABCD* operon was disrupted via a knockdown of *sitABCD* expression (see Materials and Methods and Fig. S3 for details). The growth of this mutant was very poor in the absence of added manganese (Fig. 5C), indicating an impairment in the uptake of manganese. Consistent with this conclusion, PsitA in this mutant was strongly activated at all concentrations of added manganese (45–225 nM) except for very high levels of manganese (450 nM, Fig. 5D). Altogether, these data reveal that the *sitABCD* expression under our standard conditions is essentially a response to limiting Mn in the environment. Unlike *S. typhimurium* that expresses the *sitABCD* operon (and accumulates Mn) during the lag phase, within the first 4 min of inoculation of fresh medium (Rolfe *et al.*, 2012), *R. sphaeroides* expresses the *sitABCD* operon when Mn levels in the growth medium are low (Peuser *et al.*, 2011). Our results indicate that *sitABCD* expression is only activated when Mn levels drop below a threshold of 45 nM, which is a novel finding for *R. sphaeroides*. It is not known whether *R. sphaeroides* has an additional Mn uptake system, although the presence of a general metal ion importer is plausible. Based on these results, we propose that the SitABCD system is used as an Mn scavenging strategy and conclude that the expression of this system and corresponding Mn uptake is important for growth when Mn levels in the environment are low.

#### *Polyhydroxyalkanoic acid regulation and accumulation is important for growth of R. sphaeroides*

Phasins (PhaP) are specialized proteins that bind to polyhydroxyalkanoic acid (PHA) granules and assist granule formation. Phasins may also have chaperone activities that enhance survival during stress (Mezzina and Pettinari, 2016). PHA granules are a primary form of carbon storage, and PHA granules and accompanying phasins are known to be produced by *R. sphaeroides* (Wieczorek *et al.*, 1996). *phaP* expression is regulated by its specific regulator, PhaR, during active growth (Chou *et al.*, 2009). However, the importance of PHA production

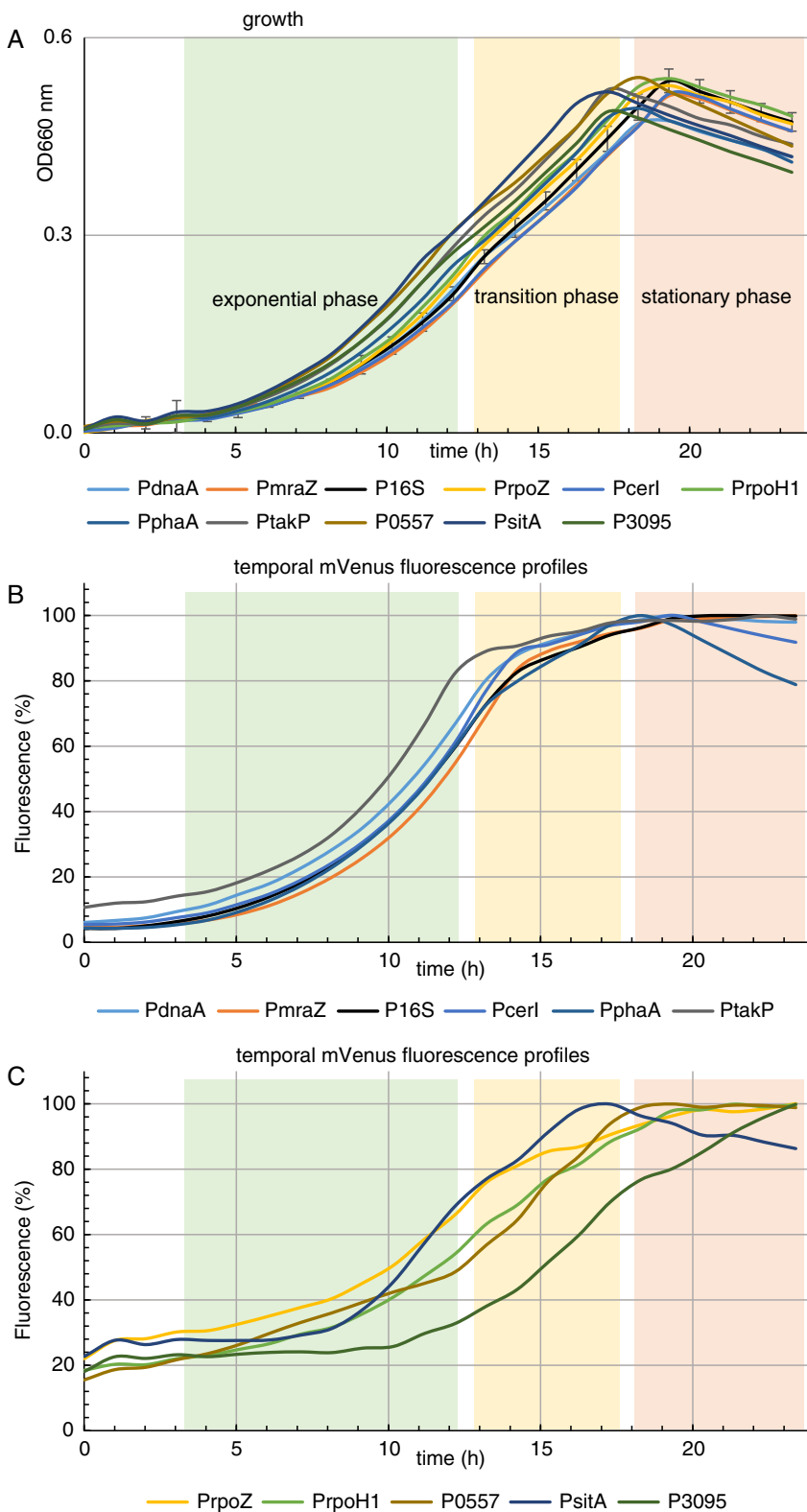


**Fig. 4.** Selected promoters fused to the gene for mVenus reveal growth phase-specific expression activity. *Rhodospirillum rubrum* wild type carrying the promoter::mVenus fusion was monitored for growth (OD<sub>660</sub>) and fluorescence during growth in a 96-well plate in defined medium diluted 1:2 with water, and grown as described in Fig. 2. A. Growth of 11 *R. sphaeroides* wild type cultures, each with a different promoter::mVenus fusion. OD is shown on a linear scale, with coloured shades representing the exponential phase (green), transitional phase (orange) and stationary phase (red). Growth under these conditions reveals a shift from exponential growth to the transition phase at approximately 12–13 h after inoculation, and a shift to stationary phase at approximately 17–19 h. Each growth curve represents the average from eight wells. To avoid confusion, the standard deviation is shown for only one growth curve. B,C. Fluorescence (F) from the promoter::mVenus fusions reveals an activity profile for each promoter over 24 h. Promoter activity is represented as percent of maximal F. Based on the shape of the activity profile, each promoter is sub-ordered to either class I (Fig. 4B), in which promoter activity was strongest during exponential growth, or class II (Fig. 4C), which contains a broad variety of promoter activity profiles which mostly increased in the transitional phase.

for the growth and survival of *R. sphaeroides* has not been elucidated. The *phaP* mRNA levels clearly increased in the transition phase and decreased in the stationary phase (Table 2, Fig. 3A and B). The PphaP

promoter fusion revealed strong activity during the exponential phase and weak activity in the transition phase (Fig. 4B). To learn if the *phaP* transcript levels were dependent upon PHA accumulation, and if PHA was

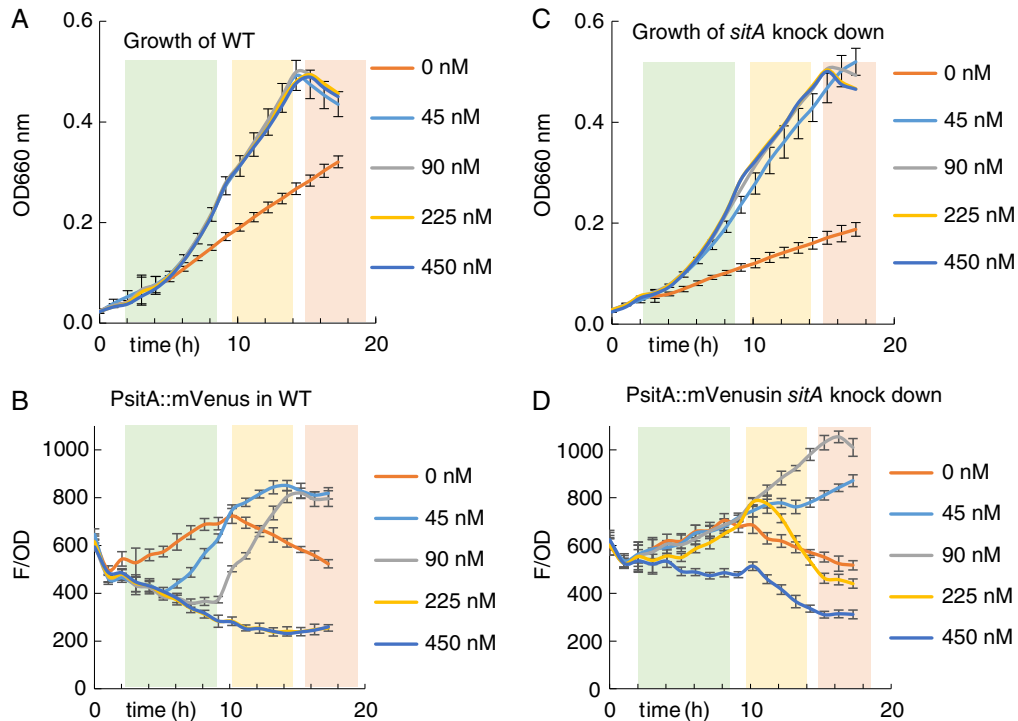


**Fig. 5.** *sitABCD* expression responds to manganese levels and is important for growth. *Rhodobacter sphaeroides* was monitored for growth and *sitABCD* expression during growth in a 96-well plate as described previously in Fig. 4. **A.** Growth of *R. sphaeroides* carrying a PsitA::mVenus fusion was monitored in a defined medium, which included all constituents (see Table S2), except for Mn. After inoculation, Mn was added at various concentrations, as indicated in the legend. Growth, represented as OD, is shown on a linear scale, with coloured shades representing the exponential phase (green), transitional phase (orange) and stationary phase (red). **B.** Expression of the *sit* operon was monitored via a fusion between the *sit* promoter region (PsitA) including the *sitA* translation start and the gene for mVenus. Expression activity from PsitA is shown as relative fluorescence (F/OD), and this reveals sensitivity to the concentration of added Mn. **C.** Growth of the *R. sphaeroides* mutant strain, in which *sitABCD* expression was knocked down via the insertion of the pK18mobII suicide vector. **D.** Relative fluorescence (F/OD) from the PsitA::mVenus fusion reveals the promoter activity in the knockdown strain is constitutively active at all concentrations of added Mn except for the highest (450 nM), indicating perturbation of manganese uptake. Error bars indicate standard deviation from eight 96-well plate cultures.

important for growth under these conditions, we generated a strain with a knockdown of expression of the PHA synthase, *phaC* (RSP\_0382), which is encoded upstream of *phaP*. Furthermore, we modified the suicide vector construct so that upon insertion into the chromosome, the native promoter of *phaC* was replaced by the promoter of the 16S ribosomal gene, ensuring constitutive *phaC* expression (see Fig. S3.) The activity of PphaP was weakened in the *phaC* knockdown strain, but enhanced in the *phaC* constitutive expression strain (Fig. 6B), indicating that *phaP* expression is dependent upon *phaC* expression. Interestingly, the expression of *phaP* was greatly weakened during growth in complex medium (Fig. 6B). Most bacteria do not accumulate PHA in complex medium. Rather, PHA synthesis and accumulation occur among all phyla of prokaryotes usually in response to nutrient limitation such as phosphorous, oxygen or nitrogen deficiency (Pötter and Steinbüchel, 2005; Jendrossek and Pfeiffer, 2014).

We monitored PHA levels using a standard method that depends upon Nile Red, a stain that is widely used to detect PHA accumulation (Lagares and Valverde,

2017). Nile Red detection of PHA accumulation confirmed that both the WT and the *phaC* constitutive expression strain accumulated significant levels of PHA during growth in defined medium, while the *phaC* knockdown strain accumulated either none or very low levels of PHA, similar to that observed in complex medium cultures (Fig. 6C). Thus, a comparison of *phaP* expression (Fig. 6B) with PHA accumulation (Fig. 6C) reveals that *phaP* expression is activated by PHA accumulation.

Finally, our results revealed that a knockdown of *phaC* expression resulted in poorer growth in defined medium but not in complex medium (Fig. 6A). Interestingly, this revealed that PHA plays an important role in supporting the growth of *R. sphaeroides* during carbon limitation, a finding that to our knowledge has never been reported in any bacterium.

#### Integration of quorum sensing and growth behaviour

Increased *cerI* mRNA levels in the transition phase (Table 2, Fig. 3A) suggested a role for quorum sensing during the adaptation to stationary phase. CerI

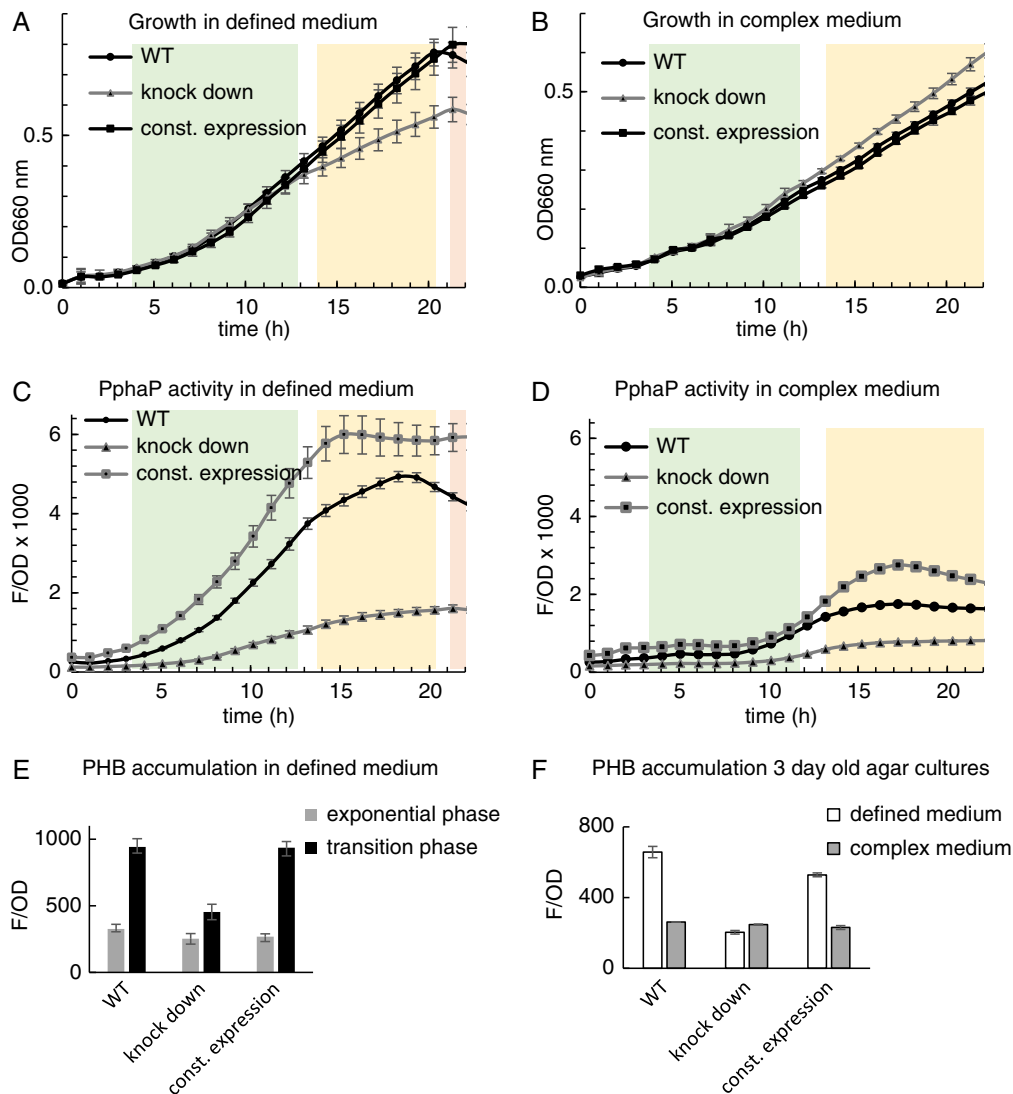


**Fig. 6.** Growth and *phaP* (phasin) expression is dependent upon PHA accumulation. *Rhodobacter sphaeroides* was monitored for growth and *phaP* expression during growth in a 96-well plate as described previously in Fig. 4. OD is shown on a linear scale, with coloured shades representing the exponential phase (green), transitional phase (orange) and stationary phase (red). The expression of *phaP* was monitored via a fusion between the *phaP* promoter and the gene for mVenus. The *R. sphaeroides* WT, a mutant strain with knockdown of expression of *phaC*, putatively coding for the PHA synthase, and a second mutant strain with constitutive expression of *phaC* (controlled by the 16S promoter) were grown in a 96-well plate with defined medium (A) as described in Fig. 4 and complex medium (B) consisting of Bacto Tryptone (1%, w/v) and yeast extract (0.05%, w/v) supplemented with  $\text{CaCl}_2$  (2 mM),  $\text{MgCl}_2$  (2 mM) and  $\text{FeSO}_4$  (43  $\mu\text{M}$ ). Growth of the knockdown strain was poorer than the WT and constitutive expression strain in defined medium but not in complex medium. C. Expression activity from the *phaP* promoter region (PphaP::mVenus fusion) during growth in defined medium was strong in the WT and constitutive expression mutant, and weak in the knockdown mutant. In complex medium, PphaP activity was weak in all strains, although a similar pattern of activity was observable. Error bars represent standard deviation from eight cultures. E. PHA accumulation was measured using the stain Nile Red in the WT and knockdown and constitutive expression mutants during growth in low aerated cultures in baffled flasks. Error bars represent standard deviation from three biological replicates. F. PHA accumulation was measured in cells harvested from defined medium agar cultures grown for 3 days. Error bars represent standard deviation from three biological replicates.

synthesizes the autoinducer signal for quorum sensing, formally known as 7,8-cis-*N*-(tetradecenyl)homoserine lactone (AHL) (Puskas *et al.*, 1997). The PcerI activity differed slightly from the transcript levels since it was only active in the exponential phase (Fig. 4B). To see how AHL levels matched with *cerI* mRNA levels and the PcerI activity profile, we used a modified *S. meliloti* strain that was previously shown to be capable of detection of AHLs

as low as 1 nM (McIntosh *et al.*, 2019). In this bacterium, the promoter activity of the AHL synthase, *sinI*, responds to the presence of AHLs. The relevant features of the *S. meliloti* AHL indicator strain (Smais) are the inability to produce AHLs via a deletion of the AHL synthase gene, *sinI*, and a fusion of the promoter of *sinI* to the mCherry fluorescent reporter gene. The addition of the supernatant from *R. sphaeroides* cultures to Smais revealed that

the levels of AHL in the *R. sphaeroides* cultures rose rapidly in the exponential phase (compare the growth curve in Fig. 7A with PcerI activity and PsinI activity in Fig. 7B). In fact, detected AHL levels in the *R. sphaeroides* wild type strain matched well with the PcerI activity (Fig. 7B). Altogether, these data suggest that the *cerI* transcript accumulates in the exponential phase and the transition phase while translation into the CerI protein and ensuing AHL accumulation occurs mostly during exponential growth.

To learn whether the Cer system was important for growth, we used the suicide vector pK18mobII to disrupt *cerI*. The *cerI* mutant showed extremely poor growth and a strongly aggregated phenotype, which was complemented by *in trans* expression of *cerI* on the plasmid pWBT (Fig. 7A). This aggregated phenotype was comparable to the previous description of a *cerI* mutant (Puskas *et al.*, 1997). We also used a similar approach to disrupt the expression of *cerR*, a *luxR*-like gene located immediately upstream of *cerI*. Based on knowledge of other QS *luxR*-*luxI* systems (Goryachev, 2009; Pappenfort and Bassler, 2016; Whiteley *et al.*, 2017), we expected CerR to be the AHL receptor and a major regulator of *cerI* expression. Indeed, disruption of *cerR* expression resulted in the loss of most of PcerI activity (Fig. 7D) and a weakly aggregated phenotype (not shown). Complementation of PcerI activity was possible via *in trans* expression of *cerR* from the plasmid pWBT (Fig. 7D). This expression from pWBT was based on the *E. coli* lac promoter, which is leaky (i.e., slightly active in the absence of the inducer, IPTG) in *R. sphaeroides* (data not shown). Remarkably, however, the leaky *in trans* expression of *cerR* resulted in complete growth arrest in liquid medium. PcerI::mVenus fluorescence could only be measured in this strain after extended growth on solid (agar) medium. The observation that *cerR* overexpression completely stalled growth in liquid culture was surprising to us, since, to our knowledge, growth-arrest via overexpression of a *luxR*-like gene has never been reported in any bacterium.

A previously proposed physiological role for the Cer (community escape response) QS system in *R. sphaeroides* is to ensure cell dispersal (Puskas *et al.*, 1997). Our results support this idea, since PcerI activity and AHL accumulation occurred primarily in growing populations (Fig. 7B). This finding fits well with the concept of QS in *R. sphaeroides* as a mechanism to ensure the dispersal of cells in growing populations rather than in stationary phase populations. The regulon of the Cer QS system has not been characterized, except for our data that confirms that the *cerI* promoter is regulated by *cerR*. However, it is plausible that the Cer system controls cell–cell attachment and polysaccharide production, since this is a reoccurring theme among the various

$\alpha$ -proteobacteria. The observation that cells grew very poorly in the absence of AHLs on one hand, and not at all upon *cerR* overexpression on the other is extremely interesting and suggests that regulation by the Cer QS extends to the control of growth and adaptation to stationary phase. This is plausible, since the AHL receptor ExpR of *S. melliloti* was also found to restrain growth specifically in the presence of AHLs and under nutrient limiting conditions (Charoenpanich *et al.*, 2015). We speculate that QS in *R. sphaeroides* and in *S. melliloti* provides a means of adapting growth behaviour in a manner analogous to the sigma factor SigB, which promotes dispersal and restrains growth within the *B. subtilis* mature biofilm (Bartolini *et al.*, 2019).

#### Alternative sigma factor RSP\_3095

Previous work has highlighted the importance of the RpoHI sigma factor during standard growth and following the transfer from the stationary phase to fresh medium (Remes *et al.*, 2017). Here, our transcriptome data revealed the expression pattern of a gene coding for another sigma factor, RSP\_3095. It had the distinction of being the only one of the 12 genes with high transcript levels in the transition phase, which continued to rise during the stationary phase under both low and highly aerated conditions (Table 2). Strong induction of alternative sigma factor expression during carbon-limited growth has been observed in another  $\alpha$ -proteobacterium, *Rhodopseudomonas palustris* (Pechter *et al.*, 2017) and the planctomycete *Rhodopirellula baltica* (Gade *et al.*, 2005). The roles of these sigma factors have not been established. We postulated that RSP\_3095 may have a role in adaptation to stationary phase, since its promoter activity is specific to the transition and stationary phases (Fig. 4C). We generated an RSP\_3095 disruptant strain using the suicide vector pK18mobII. In addition, we used pK18mobII to fuse the 16S promoter to RSP\_3095 to ensure its constitutive expression. Both of these perturbations caused a slightly slower-growing phenotype in defined liquid medium (Fig. 8A) in which the WT reached the stationary phase at 18 h after medium inoculation, while the knockdown and constitutive expression strains took 20 and 22 h, respectively. In the WT, the promoter of RSP\_3095 fused to mVenus showed little activity during exponential growth but was activated upon entry into the transition phase (Fig. 8B). In contrast, in both the knockdown and constitutive expression strains, the promoter activity remained low, suggesting that the presence of this protein is somehow important for the activity of the promoter. It is possible that the promoter of RSP\_3095 can only be activated at optimal protein levels of this sigma factor, a phenomenon that also affects regulation by RpoS in *E. coli* (Wong *et al.*, 2017). Another possibility is the cotranscription of RSP\_3094, encoding a predicted trans-membrane anti-

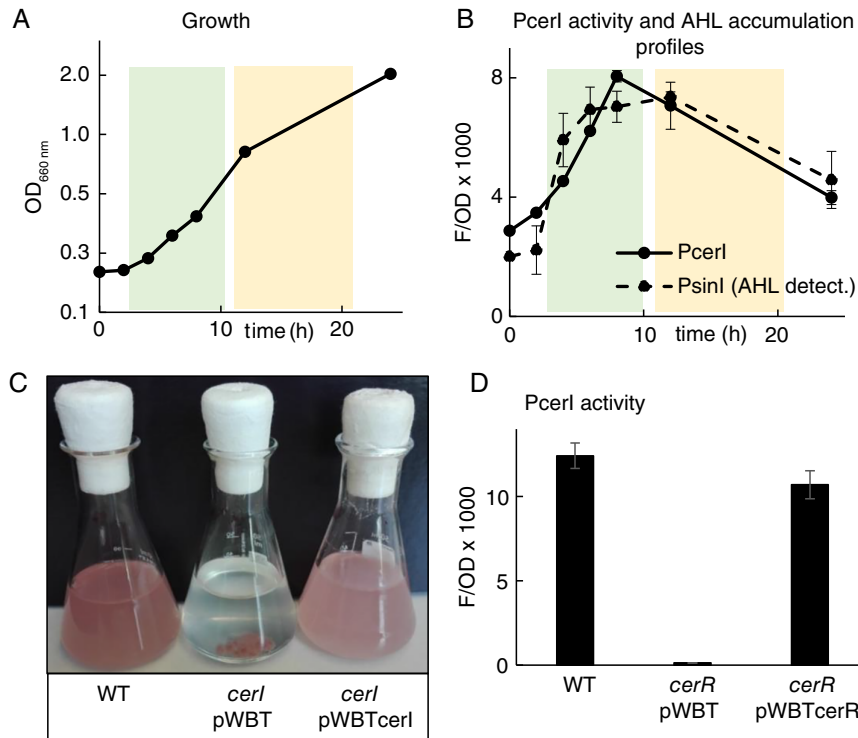


**Fig. 7.** Cer quorum sensing system is important for growth. *Rhodobacter sphaeroides* was monitored for growth (A), expression of mVenus from a PcerI::mVenus fusion (B), and AHL accumulation (B) during growth under low aerated conditions in flasks. OD 660 nm and mVenus fluorescence were taken at regular intervals. OD is shown on a linear scale, with coloured shades representing the exponential phase (green) and transitional phase (orange). For measurement of AHL accumulation, aliquots were harvested and added to the *S. meliloti* AHL indicator strain Sma15 (see materials and methods). Normalized fluorescence (F/OD) indicates the PcerI activity profile, while normalized fluorescence from PsiniI indicates the relative amount of detected AHLs. C. Flask cultures of WT and *cerI* mutant grown under low aerobic conditions for 24 h. The WT grew to an OD<sub>660 nm</sub> of almost 2.0, while the *cerI* mutant with empty vector (pWBT) grew very poorly and strongly aggregated. Constitutive *in trans* expression of *cerI* from vector pWBTcerI (Plac promoter, leaky expression) almost completely restored growth. D. Fluorescence (F/OD) from PcerI activity was measured in cells harvested from agar after growth for 48 h on complex medium agar plates. Constitutive *in trans* (leaky) expression of *cerR* from pWBTcerR prevented growth in defined medium (data not shown). PcerI activity was high in the WT, and very low in the *cerR* mutant carrying the empty vector pWBT, while pWBTcerR restored PcerI activity in the *cerR* mutant. Error bars represent the standard deviation from three biological replicates.

sigma factor, which is likely in the same operon as RSP\_3095, along with two other genes of unknown function, RSP\_3093 and RSP\_3092. mRNA levels from these genes also increased in the transition phase (Table S1). The insertion of the 16S promoter into the chromosome to constitutively express RSP\_3095 means that the downstream genes were likely also constitutively expressed, and this may be related to the observed poorer growth of this strain.

We note that the promoter activity of RSP\_3095 matches well with that of the translational *rpoS*::*lacZ* fusion in *E. coli* (Lange and Hengge-Aronis, 1994), i.e., activation at the end of exponential growth, prior to the stationary phase. Hence, it is plausible that RSP\_3095 has a comparable role to the RpoS of *E. coli*. RpoS activates carbon storage in the form of glycogen production in *E. coli* (Hengge-Aronis and Fischer, 1992) and regulates much of the QS regulon in *P. aeruginosa*

(Schuster *et al.*, 2004) and AHL accumulation in *P. fluorescens* (Liu *et al.*, 2018). Therefore, we tested the promoter activity of *cerI* and *phaA* in the RSP\_3095 knockdown and constitutive expression strains. However, while the slight growth defect was again observable (data not shown), neither of these promoters were greatly affected by the RSP\_3095 perturbations when the slight growth delay is taken into account (Fig. 8C and D). Altogether, these results suggest that the alternative sigma factor RSP\_3095 is important for its own promoter activation and that this expression contributes to growth under these conditions. Alternative sigma factors function as subunits of the RNA polymerase holoenzyme and assist in rapid promoter recognition during stress response pathways (Osterberg *et al.*, 2011). Thus, it would be interesting to identify the DNA recognition site of RSP\_3095 and to determine if this sigma factor recognizes other promoters throughout the *R. sphaeroides* genome.

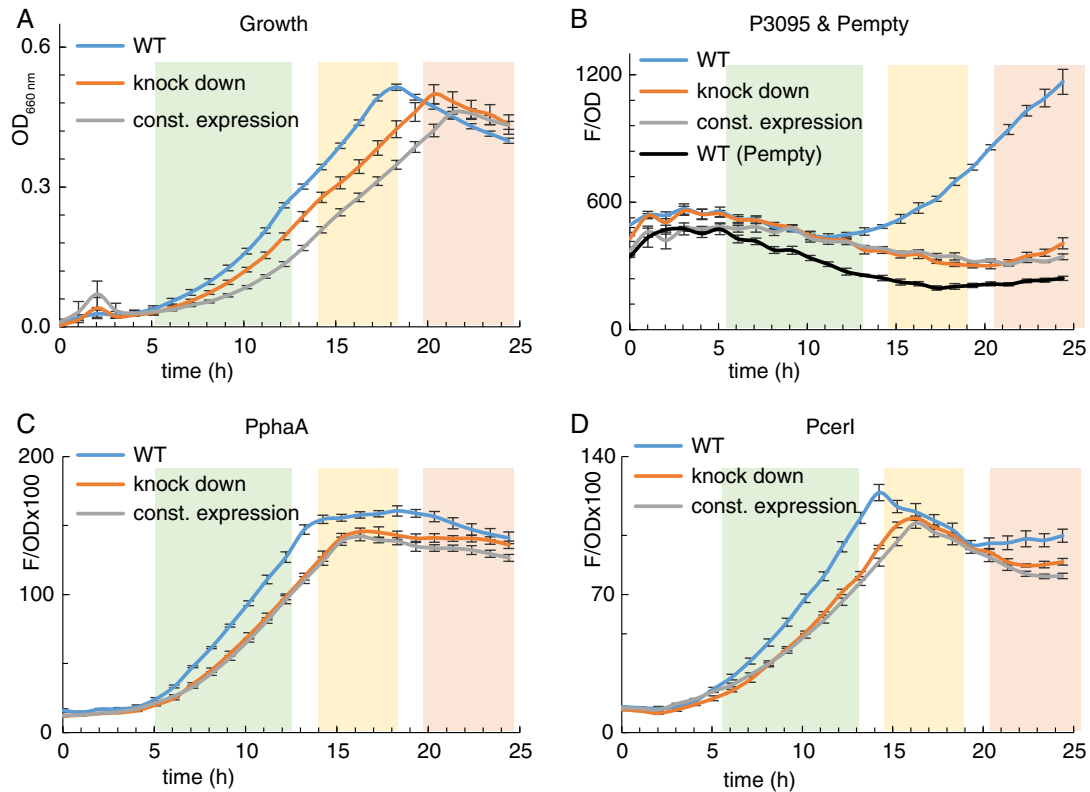


**Fig. 8.** RSP\_3095 (alternative sigma factor) controls its own expression. *Rhodobacter sphaeroides* was monitored for growth (A) and expression of mVenus from the promoter of RSP\_3095 fused to mVenus (B). OD is shown on a linear scale, with coloured shades representing the exponential phase (green), transitional phase (orange) and stationary phase (red). Growth of *R. sphaeroides* in a defined medium in a 96-well plate is affected by the knockdown or constitutive expression of RSP\_3095. B, The activity of the promoter of RSP\_3095 (P3095) is strongly decreased by either the knockdown mutation or the constitutive expression mutation, while the activity of PphaA (C) and Pcerl (D) remain unaffected. Error bars represent standard deviation from eight 96-well cultures.

#### Correlation between transcript changes and changes of the proteome in transition and early stationary phase

Microarray and RNAseq experiments outlined here provide detailed information on RNA levels of almost every gene in the genome. How does the organism translate this information into proteins from mRNAs? Discrepancies between mRNA and protein levels have been frequently noted in various organisms (Erdmann *et al.*, 2018; Bathke *et al.*, 2019). Bathke *et al.* compared the proteome under low aerated growth with the transcriptome data used in this study. The total data set is provided in Table S1. Of the transcripts that are either increased or decreased in the transition phase, the accompanying protein levels (where detected) are provided in Table 2. Correlation between transcript and protein levels was generally low but was slightly improved by comparing transition phase mRNAs with proteins accumulated in the early stationary phase (Bathke *et al.*, 2019). For example, the SitA protein showed strong accumulation, although this increase did not appear until the stationary phase (Table 2). Likewise, while the PhaP protein was detected in the transition phase, even higher levels were present at the stationary phase despite a

simultaneous decrease in the transcript levels (Table 2). In contrast, Cerl protein levels decreased strongly in the transition phase (Table 2), suggesting that the highest levels of this protein were reached in the exponential phase. Thus, while the level of *cerl* transcript increased during the transition phase (based on our microarray, RNAseq and RT-qPCR data), the *cerl* promoter activity (translation fusion with mVenus) and Cerl protein and AHLs reached their highest levels in the exponential phase and decreased in the transition phase. It is possible that the expression of *cerl* is post-transcriptionally regulated and that the stability of both Cerl protein and AHL is significantly lower than that of the *cerl* mRNA.

Many proteins were not detected in the proteomic analysis, indicative of either a high turnover and/or poor detection (e.g., through low protein solubility). Examples include the DUF1127 proteins (RSP\_6037 and RSP\_0557) and the alternative sigma factor RSP\_3095. Alternative sigma factors are known to undergo rapid proteolysis (Guo and Gross, 2014). A high turnover of RSP\_3095 might be useful for ensuring tight control of its impact on transcription activity. Notably, the protein for RSP\_3093, coding for an uncharacterized membrane protein and possibly encoded

in the same operon as RSP\_3095, was detected and its levels strongly increased in the transition phase and even further in the stationary phase (Table 2).

## Conclusions

Particularly among the  $\alpha$ -proteobacteria, how adaptation to stationary phase is regulated and coordinated is poorly understood. Our study reveals a small number of genes in *R. sphaeroides* that change their expression according to the growth phase in an oxygen-independent manner. We found that the expression of *sitABCD* (manganese uptake), *phaP* (phasin), *cerI* (quorum sensing) and RSP\_3095 (sigma factor) all play a role in normal growth in carbon limiting medium. These results reveal a considerable contrast to the  $\gamma$ -proteobacterium *E. coli* and Gram-positive *B. subtilis* and *C. glutamicum* adaptations to the stationary phase, which rely on alternative sigma factors and remodelling of the transcriptome for the adaptation to stationary phase. *Rhodobacter sphaeroides* contains multiple genes encoding sigma factors, and we showed that one of these, RSP\_3095, showed an expression profile like that of *rpoS* of *E. coli*. However, the influence of RSP\_3095 on *R. sphaeroides* growth was minimal. Rather, the largest influence on growth came from the Cer QS system. Growth was very poor in the absence of AHLs or in the presence of (weak) constitutive expression of CerR, the putative AHL receptor. These results imply that QS regulation somehow controls growth, as is the case with QS in *S. meliloti* (Charoenpanich *et al.*, 2015). Like all  $\alpha$ -proteobacteria, *S. meliloti* lacks RpoS. Instead, QS in this bacterium controls almost 9% of the transcriptome, a figure that is similar to the RpoS transcriptome of *E. coli* (Hengge, 2011). The QS regulon of the  $\gamma$ -proteobacterium *P. aeruginosa* is also comparable in size, and much of it is co-regulated by RpoS (Schuster *et al.*, 2004). Therefore, we speculate that in the absence of RpoS, the  $\alpha$ -proteobacteria may use QS to regulate at least some of the adaptation to stationary phase, such as the appropriate restraint of growth in the face of limited resources and overcrowding. However, QS alone is unlikely capable of restraining the growth of *R. sphaeroides*, since AHL accumulation occurs in the exponential phase, long before the transition to the stationary phase. It seems likely that *R. sphaeroides* adaptation to stationary phase does not rely on one major regulatory factor such as an alternative sigma factor or QS which senses environmental change and drives growth adaptation, but rather the integration and coordination of multiple factors, each capable of responding to environmental changes and impacting growth adaptation and survival. Four examples uncovered in this study are the SitABCD Mn uptake system, the production of PHA, the Cer QS system and the

RSP\_3095 alternative sigma factor. The transcript levels of genes responsible for these processes increased strongly during the transition phase, and we found that this was important for the growth of *R. sphaeroides*.

While this study focused on those genes whose transcript levels clearly change during the transition to stationary phase, we recognize that gene transcript levels and their protein products do not always correlate. Furthermore, genes whose transcripts are not upregulated in the transition phase also may play an important role in adaptation to stationary phase. For example, although the RpoH/RpoE sigma factors did not appear among our candidates with changed expression in the transition phase (see Fig. 4 for the promoter activity of *rpoH1*), deletions of these sigma factor genes cause poor growth under standard growth conditions (Nuss *et al.*, 2009; Nuss *et al.*, 2010; Remes *et al.*, 2017). Finally, our analysis did not consider all genes with increased transcript levels in the transition phase. Several other genes identified in our set-up as upregulated in the transition phase have no known function and provide interesting candidates for future studies. The novel method described in this study, which combines a suicide vector to selectively alter gene expression, promoter::reporter fusions for monitoring expression activity, and an automated assay to monitor growth and promoter activity, provides an attractive tool for elucidating the role of these uncharacterized genes.

## Materials and methods

### Bacterial strains, plasmids and growth conditions

*Rhodobacter sphaeroides* 2.4.1 and mutant derivatives are listed in Table S4, along with all the plasmids used in this study. *Rhodobacter sphaeroides* was grown at 32 °C in liquid defined medium containing malate as the carbon source (Remes *et al.*, 2014). For highly aerated growth conditions, bacteria were grown in 125 ml of medium in 500 ml Erlenmeyer baffled flasks (20% v/v) stopped with prefabricated cellulose plugs. For low aerated cultures, the conditions were comparable except that the volume of medium used in the 500 ml Erlenmeyer flasks was 400 ml (80% v/v). Flasks were constantly shaken in the dark (140 rpm). Pre-cultures that were in the exponential phase at OD<sub>660nm</sub> 0.6–0.7 were used to inoculate fresh medium to OD 0.2 to initiate the main cultures. Oxygen tension was monitored using an oximeter GMH 3610, Greisinger electronics, Germany.

### Growth in 96-well plate

For 96-well plate cultures, transparent Greiner bio-one plates were inoculated with culture (0.1 ml per well),

covered with a transparent Greiner bio-one lid with condensation rings and constantly shaken in a Tecan Infinity plate reader, incubated at 32 °C with automated measurements of optical density (OD<sub>660 nm</sub>) and fluorescence (for mVenus, ex 515 nm, em 548 nm) at 1-h intervals for up to 24 h. One important point to note with growth in a 96-well plate was the dilution of the standard minimal medium 1:2 with water. This ensured that cultures were well aerated, an important prerequisite for the maturation of the oxygen-dependent fluorescent proteins (Takahashi *et al.*, 2005; Nomata and Hisabori, 2018).

**RNA isolation and quantification** were performed as described previously (Remes *et al.*, 2017) using RT-PCR and primers listed in Table S3. Briefly, log<sub>2</sub> fold change values represent the changes in mRNA abundance at each time point (8, 11 and 28 h). This was determined by calculating the level of each target mRNA relative to that of *rpoZ* (as the reference gene) at each time point. The log<sub>2</sub> fold change was then obtained by calculating the fold change relative to the mRNA abundance in the early exponential phase (4 h). For this experiment, 8 h was near the end of the exponential phase, 11 h was in the middle of the transition phase and 28 h represents the stationary phase.

**MA, library construction and read sequencing, read mapping and coverage plot construction** have been previously described in detail (Remes *et al.*, 2017). For the construction of the MA plots, genes were only included if the detected changes in the average signal intensity [A-value:  $1/2 \log_2 (\text{Cy3} \times \text{Cy5})$ ] was above the average background signal. Amount of RNA in the exponential phase under low and highly aerated conditions was used to normalize the RNA levels at all other phases, i.e., transition phase (trans), stationary phase (stat) and outgrowth (lag), using locally weighted smoothing (LOESS) provided by the Bioconductor package Limma for R.

**Northern analysis** was performed as described previously (Berghoff *et al.*, 2009; Billenkamp *et al.*, 2015).

#### *Generation of mutants and fusion of the *cerI* promoter to mVenus*

For fusion of the promoters to mVenus, the primers for the promoter regions (Table S3) were used to amplify a fragment containing 300–400 bp upstream of each start codon plus the first 1–9 codons of the coding region. This fragment was fused to the mVenus gene in the vector pPHU231 as previously described (Charoenpanich *et al.*, 2013). For the construction of knockdown and constitutive expression mutations, ~350 bp of each gene of interest were cloned into the suicide vector pK18mobII (Schafer *et al.*, 1994) using the primers listed in Table S3. This 350 bp fragment contained the RBS,

translation start and the following nucleotides of the coding region. Located immediately downstream of this 350 bp fragment in pK18mobII was the *rpoC/thrA* tandem terminator (Harrison *et al.*, 2011). Following conjugation of the plasmid into *R. sphaeroides* using the *E. coli* strain S17-1 (Simon *et al.*, 1983), homologous recombination (single cross-over) between the cloned fragment in the suicide vector and the genomic copy of the target gene resulted in two incomplete copies of the target gene. See Fig. S3 for an explanatory diagram. The difference between knockdown and constitutive expression mutants was that the pK18mobII construct for the constitutive expression additionally contained a 113 bp fragment that contained the promoter of the 16S gene of *R. sphaeroides*, a promoter which was previously used for controlled, constitutive expression in this bacterium (Mank *et al.*, 2012). This fragment was inserted immediately upstream of the 350 bp fragment (see Fig. S3). All *R. sphaeroides* mutants and plasmids used in this study are listed in Table S4.

#### *Protein sample preparation and mass spectrometry*

Pelleted cells were harvested from liquid cultures, lysed in SDS buffer (4% w/v SDS in 0.1 M Tris/HCl, pH 7.6), heated at 70 °C for 5 min and sonicated to shear DNA. Cell debris was removed by centrifugation at 16 000g for 10 min prior to the estimation of protein concentration by DC protein assay (Bio-Rad). Solubilized proteins were precipitated by 4 volumes of acetone at –20 °C for 1 h, pelleted at 14000 g for 10 min and washed with 90% v/v acetone. Samples were dried to remove acetone completely and dissolved in urea buffer (6 M urea, 2 M thiourea, 10 mM Hepes, pH 8.0). Enzymatic fragmentation of proteins was performed by in-solution digestion (Ong and Mann, 2006). In brief, protein disulphide bonds were reduced with 1 mM dithiothreitol and alkylated with 5.5 mM iodoacetamide. Next, proteins were cleaved enzymatically by Lys-C (protein to enzyme ratio 100:1) (Wako Chemicals GmbH) at room temperature for 3 h prior to diluting samples to 2 M urea/thiourea by adding 50 mM ammonium bicarbonate. Proteins were further digested by trypsin (protein to enzyme ratio 100:1) (Promega) at room temperature overnight and the resulting mixture of peptides were desalted and concentrated by stop and go extraction (STAGE) tips (Rappsilber *et al.*, 2003).

For mass spectrometry (MS) analysis, peptides were eluted from STAGE tips by solvent B (80% v/v acetonitrile, 0.1% v/v formic acid), dried down in a SpeedVac Concentrator (Thermo Fisher Scientific) and dissolved in solvent A (0.1% v/v formic acid). Peptides were separated using a UHPLC system (EASY-nLC 1000, Thermo-Fisher Scientific) and 20 cm in-house packed C18 silica

columns (1.9  $\mu\text{m}$  C18 beads, Dr. Maisch GmbH) coupled in line to a Q-Exactive HF orbitrap mass spectrometer (ThermoFisher Scientific) using an electrospray ionization source. A gradient of 240 min was applied using linearly increasing concentration of solvent B (80% v/v acetonitrile, 0.1% v/v formic acid) over solvent A (0.1% v/v formic acid) from 5% to 30% for 215 min and from 30% to 60% for 5 min, followed by washing with 95% v/v of solvent B for 5 min and re-equilibration with 5% v/v of solvent B.

Full MS spectra were acquired in a mass range of 300–1750  $m/z$  with a resolution of 60 000 at 200  $m/z$ . The ion injection target was set to  $3 \times 10^6$  and the maximum injection time limited to 20 ms. Ions were fragmented by high-energy collision dissociation using a normalized collision energy of 27 and an ion injection target of  $5 \times 10^5$  with a maximum injection time of 20 ms. The resulting tandem mass spectra (MS/MS) were acquired with a resolution of 15 000 at 200  $m/z$  using data dependent mode with a loop count of 15 (top15).

MS raw data were processed by MaxQuant (1.5.3.12) (Cox and Mann, 2008) using the Uniprot database for *R. sphaeroides* containing 17 687 entries (release date July, 2016). The following parameters were used for data processing: Maximum of two miss cleavages, mass tolerance of 4.5 ppm for main search, trypsin as digesting enzyme, carbamidomethylation of cysteines as fixed modification, oxidation of methionine and acetylation of the protein N-terminus as variable modifications. For protein quantification, the LFQ function of MaxQuant was used. Peptides with a minimum of seven amino acids and at least one unique peptide were required for protein identification. Only proteins with at least two peptides and at least one unique peptide were considered as identified and were used for further data analysis.

#### Detection of AHLs

For the detection of AHLs, aliquots of liquid cultures were taken at regular time intervals, centrifuged to remove cells, and the supernatants were added at a 1:9 ratio to cultures of an *S. meliloti* AHL indicator strain (Smais). In this strain, the AHL synthase gene, *sinI*, is disrupted and the promoter of *sinI*, previously shown to be highly sensitive to the presence of AHLs (McIntosh et al., 2019), was fused to the gene coding for the fluorescent protein mCherry.

**RNA sequencing and analysis** was performed as previously described (Remes et al., 2014). Briefly, RNA was poly(A)-tailed and the 5' PPPs were removed using tobacco acid pyrophosphatase. RNA was then ligated to the RNA adapter. First-strand cDNA was produced from the RNA using an oligo(dT)-adapter primer and m-MLV reverse transcriptase. The cDNA was PCR-amplified, purified and then sequenced with an Illumina HiSeq machine. The adapter sequences were removed from the

sequence reads in Fastq format, and these were converted to Fasta. Read processing, generation of statistics, gene-wise read counting, reads per kilobase million (RPKM), coverage calculations and normalization were performed using READemption (Forstner et al., 2014) using *segemehl* version 0.1.3 (Hoffmann et al., 2009) for read alignments. Gene expression analysis was via DESeq 1.12.0 (Anders and Huber, 2010) and included only those genes that showed an RPKM value of  $\geq 5.0$  (Mortazavi et al., 2008). A shell script that covers the main RNAseq data processing steps is deposited at <https://zenodo.org/record/34192> (doi: 10.5281/zenodo.34192).

#### Accession number(S)

Both the microarray data and the RNAseq data are available at the NCBI GeneExpression Omnibus database under accession numbers GSE75345 and GSE71844, respectively.

#### Acknowledgements

We thank Andrea Weisert and Kerstin Habertzettl for their excellent technical assistance.

#### Conflict of Interest

None of the authors has a conflict of interest to declare.

#### Authors' contributions

K.E., M.M., B.R., and G.K. designed the experiments. K.E., M.M., B.R., and A.K. performed the experiments. M.M., K.E., and G.K. wrote the paper. All authors analysed and interpreted the data and have read and approved the final manuscript.

#### References

- Adnan, F., Weber, L., and Klug, G. (2015) The sRNA SorY confers resistance during photooxidative stress by affecting a metabolite transporter in *Rhodobacter sphaeroides*. *RNA Biol* **12**: 569–577.
- Anders, S., and Huber, W. (2010) Differential expression analysis for sequence count data. *Genome Biol* **11**: R106.
- Arai, H., Roh, J.H., and Kaplan, S. (2008) Transcriptome dynamics during the transition from anaerobic photosynthesis to aerobic respiration in *Rhodobacter sphaeroides* 2.4.1. *J Bacteriol* **190**: 286–299.
- Barnett, M.J., Bittner, A.N., Toman, C.J., Oke, V., and Long, S.R. (2012) Dual RpoH sigma factors and transcriptional plasticity in a symbiotic bacterium. *J Bacteriol* **194**: 4983–4994.
- Bartolini, M., Cogliati, S., Vileta, D., Bauman, C., Ratani, L., Lenini, C., et al. (2019) Regulation of biofilm aging and

- dispersal in *Bacillus subtilis* by the alternative sigma factor SigB. *J Bacteriol* **201**: e00473–18. <https://doi.org/10.1128/JB.00473-18>.
- Bathke, J., Konzer, A., Remes, B., McIntosh, M., and Klug, G. (2019) Comparative analyses of the variation of the transcriptome and proteome of *Rhodobacter sphaeroides* throughout growth. *BMC Genomics* **20**: 358.
- Battesti, A., Majdalani, N., and Gottesman, S. (2011) The RpoS-mediated general stress response in *Escherichia coli*. *Annu Rev Microbiol* **65**: 189–213.
- Berghoff, B.A., Glaeser, J., Sharma, C.M., Vogel, J., and Klug, G. (2009) Photooxidative stress-induced and abundant small RNAs in *Rhodobacter sphaeroides*. *Mol Microbiol* **74**: 1497–1512.
- Berghoff, B.A., Konzer, A., Mank, N.N., Looso, M., Rische, T., Forstner, K.U., et al. (2013) Integrative "omics"-approach discovers dynamic and regulatory features of bacterial stress responses. *PLoS Genet* **9**: e1003576.
- Bertrand, R.L. (2019) Lag phase is a dynamic, organized, adaptive, and evolvable period that prepares bacteria for cell division. *J Bacteriol* **201**: e00697–18. <https://doi.org/10.1128/JB.00697-18>.
- Billenkamp, F., Peng, T., Berghoff, B.A., and Klug, G. (2015) A cluster of four homologous small RNAs modulates C1 metabolism and the pyruvate dehydrogenase complex in *Rhodobacter sphaeroides* under various stress conditions. *J Bacteriol* **197**: 1839–1852.
- Blom, E.J., Ridder, A.N., Lulko, A.T., Roerdink, J.B., and Kuipers, O.P. (2011) Time-resolved transcriptomics and bioinformatic analyses reveal intrinsic stress responses during batch culture of *Bacillus subtilis*. *PLoS One* **6**: e27160.
- Cavanagh, A.T., Chandrangsu, P., and Wassarman, K. M. (2010) 6S RNA regulation of *relA* alters ppGpp levels in early stationary phase. *Microbiology* **156**: 3791–3800.
- Chang, D.E., Smalley, D.J., and Conway, T. (2002) Gene expression profiling of *Escherichia coli* growth transitions: an expanded stringent response model. *Mol Microbiol* **45**: 289–306.
- Charoenpanich, P., Meyer, S., Becker, A., and McIntosh, M. (2013) Temporal expression program of quorum sensing-based transcription regulation in *Sinorhizobium meliloti*. *J Bacteriol* **195**: 3224–3236.
- Charoenpanich, P., Soto, M.J., Becker, A., and McIntosh, M. (2015) Quorum sensing restrains growth and is rapidly inactivated during domestication of *Sinorhizobium meliloti*. *Environ Microbiol Rep* **7**: 373–382.
- Cheng, F., Ma, A., Zhuang, X., He, X., and Zhuang, G. (2016) N-(3-oxo-hexanoyl)-homoserine lactone has a critical contribution to the quorum-sensing-dependent regulation in phytopathogen *Pseudomonas syringae* pv. tabaci 11528. *FEMS Microbiol Lett* **363**: fnw265. <https://doi.org/10.1093/femsle/fnw265>.
- Chou, M.E., Chang, W.T., Chang, Y.C., and Yang, M.K. (2009) Expression of four *pha* genes involved in poly-beta-hydroxybutyrate production and accumulation in *Rhodobacter sphaeroides* FJ1. *Mol Genet Genomics* **282**: 97–106.
- Colomer-Winter, C., Flores-Mireles, A.L., Baker, S.P., Franks, K.L., Lynch, A.J.L., Hultgren, S.J., et al. (2018) Manganese acquisition is essential for virulence of *Enterococcus faecalis*. *PLoS Pathog* **14**: e1007102.
- Colomer-Winter, C., Gaca, A.O., and Lemos, J.A. (2017) Association of Metal Homeostasis and (p)ppGpp regulation in the pathophysiology of *Enterococcus faecalis*. *Infect Immun* **85**: e00260-17. <https://doi.org/10.1128/IAI.00260-17>.
- Cox, J., and Mann, M. (2008) MaxQuant enables high peptide identification rates, individualized p.p.b.-range mass accuracies and proteome-wide protein quantification. *Nat Biotechnol* **26**: 1367–1372.
- Cuny, C., Lesbats, M., and Dukan, S. (2007) Induction of a global stress response during the first step of *Escherichia coli* plate growth. *Appl Environ Microbiol* **73**: 885–889.
- de Lucena, D.K., Pühler, A., and Weidner, S. (2010) The role of sigma factor RpoH1 in the pH stress response of *Sinorhizobium meliloti*. *BMC Microbiol* **10**: 265.
- Delory, M., Hallez, R., Letesson, J.J., and De Bolle, X. (2006) An RpoH-like heat shock sigma factor is involved in stress response and virulence in *Brucella melitensis* 16M. *J Bacteriol* **188**: 7707–7710.
- Dufour, Y.S., Imam, S., Koo, B.M., Green, H.A., and Donohue, T.J. (2012) Convergence of the transcriptional responses to heat shock and singlet oxygen stresses. *PLoS Genet* **8**: e1002929.
- Elkina, D., Weber, L., Lechner, M., Burenina, O., Weisert, A., Kubareva, E., et al. (2017) 6S RNA in *Rhodobacter sphaeroides*: 6S RNA and pRNA transcript levels peak in late exponential phase and gene deletion causes a high salt stress phenotype. *RNA Biol* **14**: 1627–1637.
- Erdmann, J., Preusse, M., Khaledi, A., Pich, A., and Haussler, S. (2018) Environment-driven changes of mRNA and protein levels in *Pseudomonas aeruginosa*. *Environ Microbiol* **20**: 3952–3963.
- Fiebig, A., Herrou, J., Willett, J., and Crosson, S. (2015) General stress signaling in the Alphaproteobacteria. *Annu Rev Genet* **49**: 603–625.
- Forstner, K.U., Vogel, J., and Sharma, C.M. (2014) READemption—a tool for the computational analysis of deep-sequencing-based transcriptome data. *Bioinformatics* **30**: 3421–3423.
- Gade, D., Stuhmann, T., Reinhardt, R., and Rabus, R. (2005) Growth phase dependent regulation of protein composition in *Rhodospirella baltica*. *Environ Microbiol* **7**: 1074–1084.
- Goryachev, A.B. (2009) Design principles of the bacterial quorum sensing gene networks. *Wiley Interdiscip Rev Syst Biol Med* **1**: 45–60.
- Gregor, J., and Klug, G. (2002) Oxygen-regulated expression of genes for pigment binding proteins in *Rhodobacter capsulatus*. *J Mol Microbiol Biotechnol* **4**: 249–253.
- Guo, M.S., and Gross, C.A. (2014) Stress-induced remodeling of the bacterial proteome. *Curr Biol* **24**: R424–R434.
- Harrison, C.L., Crook, M.B., Peco, G., Long, S.R., and Griffiths, J.S. (2011) Employing site-specific recombination for conditional genetic analysis in *Sinorhizobium meliloti*. *Appl Environ Microbiol* **77**: 3916–3922.

- Hengge, R. (2009) Proteolysis of sigmaS (RpoS) and the general stress response in *Escherichia coli*. *Res Microbiol* **160**: 667–676.
- Hengge, R. (2011) Stationary-phase gene regulation in *Escherichia coli*. *EcoSal Plus* **4**. <https://doi.org/10.1128/ecosalplus.5.6.3>.
- Hengge-Aronis, R., and Fischer, D. (1992) Identification and molecular analysis of *glgS*, a novel growth-phase-regulated and *rpoS*-dependent gene involved in glycogen synthesis in *Escherichia coli*. *Mol Microbiol* **6**: 1877–1886.
- Hobbie, J.E., and Hobbie, E.A. (2013) Microbes in nature are limited by carbon and energy: the starving-survival lifestyle in soil and consequences for estimating microbial rates. *Front Microbiol* **4**: 324.
- Hoffmann, S., Otto, C., Kurtz, S., Sharma, C.M., Khaitovich, P., Vogel, J., et al. (2009) Fast mapping of short sequences with mismatches, insertions and deletions using index structures. *PLoS Comput Biol* **5**: e1000502.
- Jaishankar, J., and Srivastava, P. (2017) Molecular basis of stationary phase survival and applications. *Front Microbiol* **8**: 2000.
- Jendrossek, D., and Pfeiffer, D. (2014) New insights in the formation of polyhydroxyalkanoate granules (carboxosomes) and novel functions of poly(3-hydroxybutyrate). *Environ Microbiol* **16**: 2357–2373.
- Katayama, T., Ozaki, S., Keyamura, K., and Fujimitsu, K. (2010) Regulation of the replication cycle: conserved and diverse regulatory systems for DnaA and oriC. *Nat Rev Microbiol* **8**: 163–170.
- Kehres, D.G., and Maguire, M.E. (2003) Emerging themes in manganese transport, biochemistry and pathogenesis in bacteria. *FEMS Microbiol Rev* **27**: 263–290.
- Krol, E., and Becker, A. (2011) ppGpp in *Sinorhizobium meliloti*: biosynthesis in response to sudden nutritional downshifts and modulation of the transcriptome. *Mol Microbiol* **81**: 1233–1254.
- Lagares, Jr., A., and Valverde, C. (2017) Quantification of bacterial Polyhydroxybutyrate content by flow Cytometry. *Bio-Protoc* **7**: e2638. <https://doi.org/10.21769/BioProtoc.2638>.
- Lange, R., and Hengge-Aronis, R. (1994) The cellular concentration of the sigma(S) subunit of RNA-polymerase in *Escherichia coli* is controlled at the levels of transcription translation, and protein stability. *Genes Dev* **8**: 1600–1612.
- Li, Q., Peng, T., and Klug, G. (2018) The PhyR homolog RSP\_1274 of *Rhodobacter sphaeroides* is involved in defense of membrane stress and has a moderate effect on RpoE (RSP\_1092) activity. *BMC Microbiol* **18**: 18.
- Liu, X., Ji, L., Wang, X., Li, J., Zhu, J., and Sun, A. (2018) Role of RpoS in stress resistance, quorum sensing and spoilage potential of *Pseudomonas fluorescens*. *Int J Food Microbiol* **270**: 31–38.
- Mank, N.N., Berghoff, B.A., Hermanns, Y.N., and Klug, G. (2012) Regulation of bacterial photosynthesis genes by the small noncoding RNA PcrZ. *Proc Natl Acad Sci U S A* **109**: 16306–16311.
- Martinez-Salazar, J.M., Sandoval-Calderon, M., Guo, X., Castillo-Ramirez, S., Reyes, A., Loza, M.G., et al. (2009) The *Rhizobium etli* RpoH1 and RpoH2 sigma factors are involved in different stress responses. *Microbiology* **155**: 386–397.
- McIntosh, M., Serrania, J., and Lacanna, E. (2019) A novel LuxR-type solo of *Sinorhizobium meliloti*, NurR, is regulated by the chromosome replication coordinator, DnaA, and activates quorum sensing. *Mol Microbiol* **112**: 678–698.
- Mezzina, M.P., and Pettinari, M.J. (2016) Phasins, multifaceted Polyhydroxyalkanoate granule-associated proteins. *Appl Environ Microbiol* **82**: 5060–5067.
- Mika, F., and Hengge, R. (2013) Small regulatory RNAs in the control of motility and biofilm formation in *E. coli* and *Salmonella*. *Int J Mol Sci* **14**: 4560–4579.
- Mortazavi, A., Williams, B.A., McCue, K., Schaeffer, L., and Wold, B. (2008) Mapping and quantifying mammalian transcriptomes by RNA-Seq. *Nat Methods* **5**: 621–628.
- Navarro Llorens, J.M., Tormo, A., and Martinez-Garcia, E. (2010) Stationary phase in gram-negative bacteria. *FEMS Microbiol Rev* **34**: 476–495.
- Nomata, J., and Hisabori, T. (2018) Development of heme protein based oxygen sensing indicators. *Sci Rep* **8**: 11849.
- Nuss, A.M., Glaeser, J., Berghoff, B.A., and Klug, G. (2010) Overlapping alternative sigma factor regulons in the response to singlet oxygen in *Rhodobacter sphaeroides*. *J Bacteriol* **192**: 2613–2623.
- Nuss, A.M., Glaeser, J., and Klug, G. (2009) RpoH (II) activates oxidative-stress defense systems and is controlled by RpoE in the singlet oxygen-dependent response in *Rhodobacter sphaeroides*. *J Bacteriol* **191**: 220–230.
- Nystrom, T. (2003) Conditional senescence in bacteria: death of the immortals. *Mol Microbiol* **48**: 17–23.
- Ong, S.E., and Mann, M. (2006) A practical recipe for stable isotope labeling by amino acids in cell culture (SILAC). *Nat Protoc* **1**: 2650–2660.
- Ortiz, C., Natale, P., Cueto, L., and Vicente, M. (2016) The keepers of the ring: regulators of FtsZ assembly. *FEMS Microbiol Rev* **40**: 57–67.
- Osterberg, S., del Peso-Santos, T., and Shingler, V. (2011) Regulation of alternative sigma factor use. *Annu Rev Microbiol* **65**: 37–55.
- Papenfort, K., and Bassler, B.L. (2016) Quorum sensing signal-response systems in Gram-negative bacteria. *Nat Rev Microbiol* **14**: 576–588.
- Patek, M., and Nesvera, J. (2011) Sigma factors and promoters in *Corynebacterium glutamicum*. *J Biotechnol* **154**: 101–113.
- Pechter, K.B., Yin, L., Oda, Y., Gallagher, L., Yang, J., Manoil, C., and Harwood, C.S. (2017) Molecular basis of bacterial longevity. *MBio* **8**: e01726–17. <https://doi.org/10.1128/mBio.01726-17>.
- Peuser, V., Metz, S., and Klug, G. (2011) Response of the photosynthetic bacterium *Rhodobacter sphaeroides* to iron limitation and the role of a Fur orthologue in this response. *Environ Microbiol Rep* **3**: 397–404.
- Pötter, M., and Steinbüchel, A. (2005) Poly(3-hydroxybutyrate) granule-associated proteins: impacts on poly(3-hydroxybutyrate) synthesis and degradation. *Bio-macromolecules* **6**: 552–560.

- Prossliner, T., Skovbo Winther, K., Sorensen, M.A., and Gerdes, K. (2018) Ribosome hibernation. *Annu Rev Genet* **52**: 321–348.
- Puskas, A., Greenberg, E.P., Kaplan, S., and Schaefer, A.L. (1997) A quorum-sensing system in the free-living photosynthetic bacterium *Rhodobacter sphaeroides*. *J Bacteriol* **179**: 7530–7537.
- Rappsilber, J., Ishihama, Y., and Mann, M. (2003) Stop and go extraction tips for matrix-assisted laser desorption/ionization, nanoelectrospray, and LC/MS sample pretreatment in proteomics. *Anal Chem* **75**: 663–670.
- Remes, B., Berghoff, B.A., Forstner, K.U., and Klug, G. (2014) Role of oxygen and the OxyR protein in the response to iron limitation in *Rhodobacter sphaeroides*. *BMC Genomics* **15**: 794.
- Remes, B., Rische-Grahl, T., Muller, K.M.H., Forstner, K.U., Yu, S.H., Weber, L., et al. (2017) An RpoHI-dependent response promotes outgrowth after extended stationary phase in the Alphaproteobacterium *Rhodobacter sphaeroides*. *J Bacteriol* **199**: e00249–17. <https://doi.org/10.1128/JB.00249-17>.
- Rolfe, M.D., Rice, C.J., Lucchini, S., Pin, C., Thompson, A., Cameron, A.D., et al. (2012) Lag phase is a distinct growth phase that prepares bacteria for exponential growth and involves transient metal accumulation. *J Bacteriol* **194**: 686–701.
- Roop, R.M., 2nd, Gee, J.M., Robertson, G.T., Richardson, J. M., Ng, W.L., and Winkler, M.E. (2003) Brucella stationary-phase gene expression and virulence. *Annu Rev Microbiol* **57**: 57–76.
- Schafer, A., Tauch, A., Jager, W., Kalinowski, J., Thierbach, G., and Pühler, A. (1994) Small mobilizable multi-purpose cloning vectors derived from the *Escherichia coli* plasmids pK18 and pK19: selection of defined deletions in the chromosome of *Corynebacterium glutamicum*. *Gene* **145**: 69–73.
- Schuster, M., Hawkins, A.C., Harwood, C.S., and Greenberg, E.P. (2004) The *Pseudomonas aeruginosa* RpoS regulon and its relationship to quorum sensing. *Mol Microbiol* **51**: 973–985.
- Sedlyarova, N., Shamovsky, I., Bharati, B.K., Epshtein, V., Chen, J., Gottesman, S., et al. (2016) sRNA-mediated control of transcription termination in *E. coli*. *Cell* **167**: 111–121.e13.
- Simon, R., Priefer, U., and Pühler, A. (1983) A broad host range mobilization system for in vivo genetic engineering: transposon mutagenesis in Gram-negative bacteria. *Bio-technology* **1**: 784–791.
- Staron, A., and Mascher, T. (2010) General stress response in alpha-proteobacteria: PhyR and beyond. *Mol Microbiol* **78**: 271–277.
- Takahashi, E., Takano, T., Numata, A., Hayashi, N., Okano, S., Nakajima, O., et al. (2005) Genetic oxygen sensor: GFP as an indicator of intracellular oxygenation. *Adv Exp Med Biol* **566**: 39–44.
- Testerman, T.L., Vazquez-Torres, A., Xu, Y., Jones-Carson, J., Libby, S.J., and Fang, F.C. (2002) The alternative sigma factor sigmaE controls antioxidant defences required for *Salmonella* virulence and stationary-phase survival. *Mol Microbiol* **43**: 771–782.
- Weiss, A., Broach, W.H., and Shaw, L.N. (2016) Characterizing the transcriptional adaptation of *Staphylococcus aureus* to stationary phase growth. *Pathog Dis* **74**: 541–554. <https://doi.org/10.1093/femsre/fuv005>.
- Weiss, A., and Shaw, L.N. (2015) Small things considered: the small accessory subunits of RNA polymerase in Gram-positive bacteria. *FEMS Microbiol Rev* **39**: 541–554.
- Whiteley, M., Diggle, S.P., and Greenberg, E.P. (2017) Progress in and promise of bacterial quorum sensing research. *Nature* **551**: 313–320.
- Wieczorek, R., Steinbuchel, A., and Schmidt, B. (1996) Occurrence of polyhydroxyalkanoic acid granule-associated proteins related to the *Alcaligenes eutrophus* H16 GA24 protein in other bacteria. *FEMS Microbiol Lett* **135**: 23–30.
- Wong, G.T., Bonocora, R.P., Schep, A.N., Beeler, S.M., Lee Fong, A.J., Shull, L.M., et al. (2017) Genome-wide transcriptional response to varying RpoS levels in *Escherichia coli* K-12. *J Bacteriol* **199**: e00755–16. <https://doi.org/10.1128/JB.00755-16>.
- Yang, C.K., Tai, P.C., and Lu, C.D. (2014) Time-related transcriptome analysis of *B. subtilis* 168 during growth with glucose. *Curr Microbiol* **68**: 12–20.
- Zeilstra-Ryalls, J.H., and Kaplan, S. (2004) Oxygen intervention in the regulation of gene expression: the photosynthetic bacterial paradigm. *Cell Mol Life Sci* **61**: 417–436.

### Supporting Information

Additional Supporting Information may be found in the online version of this article at the publisher's web-site:

**Appendix S1:** Supporting Information 1

**Appendix S2:** Supporting Information 2